APPENDIX

A1

Štiavnická M., García-Álvarez O., Ulčová-Gallová Z., Sutovsky P., Abril-Parreño L., Dolejšová M., Řimnáčová H., Moravec J., Hošek P., Lošan P., Gold L., Fenclová T., Králíčková M., Nevoral J. 2020. H3K4me2 accompanies chromatin immaturity in human spermatozoa: an epigenetic marker for sperm quality assessment. Syst Biol Reprod Med. 66(1):3-11. doi: 10.1080/19396368.2019.1666435. (**IF_{2020} = 3.061**)

Taylor & Francis
Taylor & Francis Group

Systems Biology in Reproductive Medicine

ISSN: 1939-6368 (Print) 1939-6376 (Online) Journal homepage: https://www.tandfonline.com/loi/iaan20

H3K4me2 accompanies chromatin immaturity in human spermatozoa: an epigenetic marker for sperm quality assessment

Miriama Štiavnická, Olga García-Álvarez, Zděnka Ulčová-Gallová, Peter Sutovsky, Laura Abril-Parreño, Martina Dolejšová, Hedvika Řimnáčová, Jiří Moravec, Petr Hošek, Petr Lošan, Lukáš Gold, Tereza Fenclová, Milena Králíčková & Jan Nevoral

To cite this article: Miriama Štiavnická, Olga García-Álvarez, Zděnka Ulčová-Gallová, Peter Sutovsky, Laura Abril-Parreño, Martina Dolejšová, Hedvika Řimnáčová, Jiří Moravec, Petr Hošek, Petr Lošan, Lukáš Gold, Tereza Fenclová, Milena Králíčková & Jan Nevoral (2020) H3K4me2 accompanies chromatin immaturity in human spermatozoa: an epigenetic marker for sperm quality assessment, Systems Biology in Reproductive Medicine, 66:1, 3-11, DOI: 10.1080/19396368.2019.1666435

To link to this article: https://doi.org/10.1080/19396368.2019.1666435

Published online: 03 Oct 2019.

SYSTEMS BIOLOGY IN REPRODUCTIVE MEDICINE
2020, VOL. 66, NO. 1, 3–11
https://doi.org/10.1080/19396368.2019.1666435

Taylor & Francis
Taylor & Francis Group

RESEARCH COMMUNICATION

H3K4me2 accompanies chromatin immaturity in human spermatozoa: an epigenetic marker for sperm quality assessment

Miriama Štiavnická[a], Olga García-Álvarez[a,b*#], Zděnka Ulčová-Gallová[c,d], Peter Sutovsky[e,f*], Laura Abril-Parreño[a,g], Martina Dolejšová[a], Hedvika Řimnáčová[a], Jiří Moravec[a], Petr Hošek[a], Petr Lošan[c], Lukáš Gold[a], Tereza Fenclová[a], Milena Králíčková[a,h*], and Jan Nevoral[a,h*]

[a]Biomedical Center in Pilsen, Faculty of Medicine in Pilsen, Charles University, Pilsen, Czech Republic; [b]Health and Biotechnology (SaBio) GroupIREC, (CSIC-UCLM-JCCM), Albacete, Spain; [c]Genetika Plzeň, s.r.o. (Ltd.), Pilsen – Černice, Czech Republic; [d]Department of Gynecology and Obstetrics, Charles University, Pilsen, Czech Republic; [e]Division of Animal Sciences, University of Missouri, Columbia, MO, USA; [f]Department of Obstetrics, Gynecology and Women's Health, University of Missouri, Columbia, MO, USA; [g]Laboratory of Animal Reproduction, Department of Biological Sciences, University of Limerick, Limerick, Irelan; [h]Department of Histology and Embryology, Faculty of Medicine in Pilsen, Charles University, Plzeň, Czech Republic

ABSTRACT

Chromatin remodeling, including histone post-translational modifications, during spermatogenesis can affect sperm quality and fertility, and epigenetic marks may therefore be useful for clinical evaluations of sperm. Together with histone hyperacetylation, the dimethylation of histone H3 on lysine K4 (H3K4me2) is also required during protamination. Accordingly, we evaluated the utilization of this epigenetic mark for the identification of sperm with decrease quality and immature chromatin. In this study, 99 semen samples, including 22 normozoospermic (N), 63 asthenozoospermic (A), and 14 oligoasthenozoospermic (OA) samples, were comprehensively analyzed with respect to H3K4me2 levels, DNA damage (DNA fragmentation index, DFI), and sperm immaturity (high DNA stainability, %HDS), as determined by a sperm chromatin structure assay using flow cytometry. We detected a significant relationship between H3K4me2 and %HDS ($r = 0.47$; $p < 0.001$). Furthermore, we observed negative correlations between H3K4me2 and sperm concentration, motility, and mitochondrial activity ($p < 0.05$). The increase in immaturity as semen quality decreased (N > A > OA) indicates the importance of chromatin immaturity and histone code deviations in sperm evaluations. Using various approaches, our study elucidated H3K4me2 as a molecular marker of sperm quality with potential use in reproductive medicine.

Abbreviations: A: asthenozoospermic; AO: acridine orange; ART: assisted reproductive therapy; BWW: Biggers-Whitten Whittingham; DAPI: 4′,6′ -diamidino-2-phenylindole; DFI: DNA fragmentation index; H3K4me2: dimethylation of lysine K4 on histones H3; HDS: high DNA stainability; HRP: horseradish peroxidase; MACS: magnetic-activated cell sorting; N: normospermic; NGS: normal goat serum; OA: oligoasthenozoospermic; PTM: post-translational modification; SCSA: sperm chromatin structure assay; SUTI: sperm ubiquitin tag assay; TBS-T: TBS with 0.5% Tween-20

ARTICLE HISTORY
Received 15 May 2019
Revised 28 August 2019
Accepted 8 September 2019

KEYWORDS
Sperm DNA; H3K4me2; epigenetics; chromatin immaturity; high DNA stainability

Introduction

To successfully deliver genetic and epigenetic information in the sperm to an embryo, the chromatin has to be hyper-condensed to protect the paternal DNA and epigenome against various external factors (Oliva 2006; Carrell et al. 2007; Castillo et al. 2011). This is ensured by histone replacement with protamines by sperm DNA protamination (Balhorn 2007). Despite this, a minute amount of histones retained in the sperm head undergo various post-translational modifications (PTMs) (Rathke et al. 2014; Luense et al. 2016; Eelaminejad et al. 2017). In addition to sperm DNA methylation and non-coding RNA cargo, the histone code contributes to the epigenetic signature of the spermatozoon, to help regulate early post-fertilization events and embryonic development (van der Heijden et al. 2008; Hammoud et al. 2011; La Spina et al. 2014; Sharma et al. 2018; Schon et al. 2019). Chromatin remodeling during spermatogenesis is quite sensitive to environmental conditions, and exposure to oxidative stress is the most common explanation for decreased sperm quality, as determined by accessibility to DNA fragmentation or apoptosis (Tavalaee et al. 2009; Tunc

CONTACT Olga García-Álvarez olga.garcia@uclm.es Biomedical Center in Pilsen, Faculty of Medicine in Pilsen, Charles University, Alej Svobody 1655/76, Pilsen 323 00, Czech Republic
#Present address: Health and Biotechnology (SaBio) Group, IREC (CSIC-UCLM- JCCM). Campus Universitario s.n. 02071, Albacete, Spain
*Senior co-authors

and Tremellen 2009; Bahreinian et al. 2015). Accordingly, aberrations in sperm chromatin, including histone PTMs, could be related to a decrease in sperm quality, defined by conventional semen parameters or mitochondria activity (Kiani-Esfahani et al. 2013). Although the physiological roles of several histone PTMs have been deciphered, a detailed understanding of epigenetic patterns in sperm is lacking (Aoki et al. 2005; Siklenka et al. 2015; Zhong et al. 2015; Pérez- Cerezales et al. 2017). Therefore, investigations of the sperm chromatin histone code may lead to improve- ments in assisted reproductive therapy (ART).

Dimethylation of lysine K4 on histones H3 (H3K4me2) is well-studied in sperm and is a candidate fertility-related histone PTM for several reasons. i) Together with H4 hyperacetylation, H3K4me2 participates in chromatin opening, required for histone-protamine exchange (Rathke et al. 2007). ii) The incidence of H3K4me2 is highest in the final stages of spermiogenesis, coinciding with protamination and acrosome formation (Godmann et al. 2007). iii) H3K4me2 has been detected at the promoters of transcriptionally active housekeeping genes and genes indispensable for spermatogenesis (Brykczynska et al. 2010), and an excess or lack of modification could be responsible for aberrant early embryogenesis (Aoshima et al. 2015). iv) Paternal H3K4me2 is involved in the regulation of gene expression during early embryonic development (Teperek et al. 2016) and the loss of H3K4me2 is paternally inherited across generations (Siklenka et al. 2015).

H3K4me2 has the potential to be a marker of sperm quality, with implications for improving ART. Therefore, we hypothesize that defects in chromatin integrity and pathological sperm quality are associated with an excess of H3K4me2 modification.

Results and discussion

To examine the role of H3K4me2 as an epigenetic marker of human sperm quality, we used sperm samples classified as normospermic (N), asthenozoospermic (A), and oligoasthenozoospermic (OA) according to the WHO (World Health Organization 2010) and evaluated the following semen parameters: age, volume, sperm concentration, total and progressive motility, mitochondrial activity/early apoptotic spermatozoa, and chromatin immaturity (expressed as %HDS). As expected, all sperm features other than volume differed significantly among groups (Table 1). These parameters also differed when samples were divided into those with low %HDS (HDS ≤ 15) and high %HDS (HDS > 15) (Table 2) according to Evenson (2011). The concentration of spermatozoa and sperm motility within the HDS < 15 – samples was greater. However, there were no significant differences in mitochondrial activity or, surprisingly, DNA damage (expressed as %DFI) between HDS groups, despite a significant correlation between HDS and DFI (r = 0.200 p = 0.047) (Table 3).

Immature sperm in the ejaculate is usually explained by the premature release of spermatids from seminiferous tubules in testes before they fully differentiate (Yeung et al. 2007; Talebi et al. 2008; Elshal et al. 2009). Specific

Table 2. Overview of sperm parameters according to the HDS.

	%HDS ≤ 15 (69)	%HDS > 15 (30)	p-value
Age (years)	36 (32–39)	34.5 (31–39)	0.278
Volume (ml)	3.30 (2.40–4.50)	3.00 (2.50–3.20)	0.101
Concentration (mil/ml)	57.00 (29.00–86.00)	31.50 (18.00–70.00)	0.046
Total motility	52.00 (42.00–65.00)	49.00 (33.00–61.00)	0.041
Progressive motility	11.00 (5.00–24.00)	6.00 (0.00–16.00)	0.043
MitoTracker+/YO-PRO1- (%)	61.00 (49.50–71.23)	52.45 (39.50–66.92)	0.067
MitoTracker-/YO-PRO1+ (%)	19.29 (14.18–28.90)	23.33 (18.49–34.52)	0.180
%DFI	11.59 (7.35–18.41)	13.45 (11.03–19.31)	0.124

Values are expressed as medians (quartiles) and as significant are considered differences at $p < 0.05$. HDS, High DNA stainability; DFI, DNA fragmentation index. Numbers of patients in the group with low and high HDS are indicated above each column.

Table 3. Summary of Spearman's rank correlations between % HDS and other sperm parameters.

	%HDS	p-value
Age (years)	−0.125	0.220
Volume (ml)	−0.072	0.480
Concentration (mil/ml)	−0.331	<0.001
Total motility (%)	−0.270	0.007
Progressive motility (%)	−0.310	0.002
MitoTracker+/YO-PRO1- (%)	−0.261	0.023
MitoTracker-/YO-PRO1+ (%)	0.171	0.140
%DFI	0.200	0.047

Correlations are considered significant at $p < 0.05$. HDS, high DNA stainability index; DFI, DNA fragmentation index.

Table 1. Overview of sperm parameters according to semen quality.

	N (22)	A (63)	OA (14)	p-value
Age (years)	34 (31–37)[ab]	36 (33–40)[a]	32.5 (31–37)[b]	0.037
Volume (ml)	2.70 (2.10–3.40)[a]	3.15 (2.50–4.20)[a]	3.50 (2.40–5.10)[a]	0.139
Concentration (mil/ml)	84.00 (69.00–109.00)[a]	49.00 (29.00–78.00)[b]	7.00 (4.00–10.00)[c]	<0.001
Total motility (%)	66.00 (64.00–73.00)[a]	49.00 (37.00–56.00)[b]	42.00 (36.00–56.00)[b]	<0.001
Progressive motility (%)	37.50 (30.00–50.00)[a]	8.00 (3.00–14.00)[b]	0.00 (0.00–10.00)[b]	<0.001
% HDS	6.87 (3.98–10.09) [a]	10.43 (6.63–18.32)[a]	11.77 (5.52–30.38)[a]	0.044
MitoTracker+/YO-PRO1- (%)	71.31 (63.65–84.33) [a]	53.94 (43.50–66.37) [b]	51.095 (38.95–57.94) [b]	0.001
MitoTracker-/YO-PRO1+ (%)	14.05 (9.76–18.41) [a]	22.78 (17.18–30.89) [b]	24,17 (20.59–30.47) [b]	0.004

Values are expressed as medians (quartiles). Different superscript letters within a row denote significant differences ($p < 0.05$). N, normozoospermic; A, asthenozoospermic; OA, oligoasthenozoospermic; % HDS, high DNA stainability index. Numbers of patients in N, A, and OA groups are indicated above each column.

Table 4. Summary of Spearman's rank correlations between H3K4me2 and other sperm parameters.

	H3K4me2	*p*-value
Age (years)	−0.120	0.261
Volume (ml)	0.120	0.260
Concentration (mil/ml)	−0.570	<0.001
Total motility (%)	−0.093	0.374
Progressive motility (%)	−0.250	0.015
MitoTracker+/YO-PRO1- (%)	−0.175	0.140
MitoTracker-/YO-PRO1+ (%)	0.010	0.410
%DFI	0.162	0.120
%HDS	0.470	<0.001

Correlations are considered significant at $p < 0.05$. HDS, high DNA stainability index; DFI, DNA fragmentation index.

treatments for testicular cancer can also increase the presence of immature sperm (Maselli et al. 2012), and this may reconcile the residual histones and the abundance of PTMs in semen samples displaying chromatin immaturity. Various PTMs of canonical histones affect residual histones in sperm and have crucial roles with respect to several specific properties of the spermatozoon: the replacement of most core histones *via* protamination, transcriptional inactivity, and a haploid genome designed for fusion with oocytes. Therefore, the sperm histone code is an important determinant of sperm fertilization ability and the destiny of paternal chromatin in embryos (Nevoral and Sutovsky 2017). Moreover, the histone code is sensitive to the environment, which influences sperm quality via epigenetic mechanisms (Delbes et al. 2010; Jenkins et al. 2017; Gunes et al. 2018). Lysine (K) di- and trimethylation of sperm histones are frequent PTMs promoting gene silencing and chromatin protection (van der Heijden et al. 2006; Hammoud et al. 2009, 2011; Brykczynska et al. 2010; Siklenka et al. 2015). However, the degree of methylation of H3 on lysine K4 has greater effects (i.e., transcriptional repression or activation) than those of the methylation of other lysine residues. Consequently, H3K4me2 that is a coincident marker for transcription factor binding sites was used to evaluate human sperm physiology in this study (visualized *in situ* on Figure 1A).

We found a positive association between the H3K4me2 level and sperm chromatin immaturity (%HDS) ($r = 0.470$; $p < 0.001$) (Table 3). Moreover,

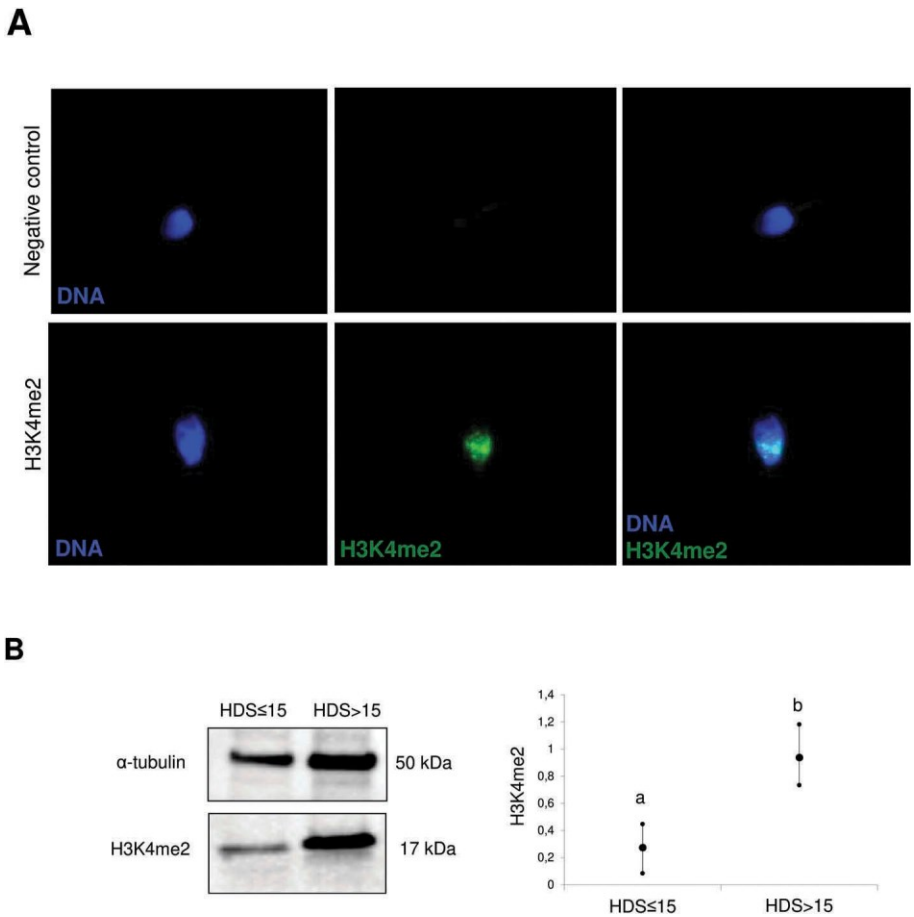

Figure 1. Representative images of the subcellular localization of H3K4me2 in sperm. A) Immunocytochemical localization of H3K4me2 and negative control. B) Difference in H3K4me2 abundance between high and low HDS samples, as determined by western blot densitometry, with an anti-alpha tubulin antibody as a loading control. The data are expressed as means, including min–max whiskers, and different superscripts indicate statistical significance ($p < 0.05$). HDS, high DNA stainability index.

there were significant differences between groups classified by %HDS in H3K4me2 levels, as assessed by flow cytometry (Figure 2A,B,D). The specificity of the H3K4me2 antibody and its localization to the nucleus were confirmed by immunofluorescence and western blotting (Figure 1A,B). Increased dimethylated H3K4 occurs in elongating spermatids undergoing nuclear protamination (Godmann et al. 2007), and the H3K4me2 modification plays a role in chromatin open- ing, required for histone replacement by protamines (Rathke et al. 2007). Altogether, H3K4me2 in sperma- tozoa has clinical value and could be used to explain preimplantation failure after ART (Speyer et al. 2015), presumably due to the contribution on embryonic gene expression (Hammoud et al. 2009, 2011; Aoshima et al. 2015). Furthermore, H3K4me2 levels were correlated with sperm concentration and motility (Table 4) and were significantly higher for OA and A samples than for N samples (Figure 2C), emphasizing its value for sperm quality assessment and description.

Many studies have found evidence for decreases in concentration and motility in spermatozoa with incom- plete protamination (Aoki et al. 2005; La Spina et al. 2014), consistent with our H3K4me2 results indicating significant correlations with sperm concentration, motility, and % HDS. A correlation was observed between incomplete chromatin condensation and sperm quality parameters, such as concentration, motility, and mitochondrial activity (Table 3). Despite a lack of significant differences in %HDS between groups with different semen qualities (Figure 3), we detected a significant relationship ($r = 0.232$; $p = 0.021$) between increasing %HDS and decreasing semen quality (N > A > OA). Indeed, spermatozoa with high chromatin immaturity (%HDS) did not exhibit successful chromatin condensation and are more vulnerable to oxidative stress, DNA fragmentation, and apoptosis (Tunc and Tremellen 2009; Bahreinian et al. 2015). However, even at levels of high %HDS, an increase in %DFI was not observed (similar to the results of our analysis of HDS groups), but a specific histones were concomitantly up-regulated (Maselli et al.

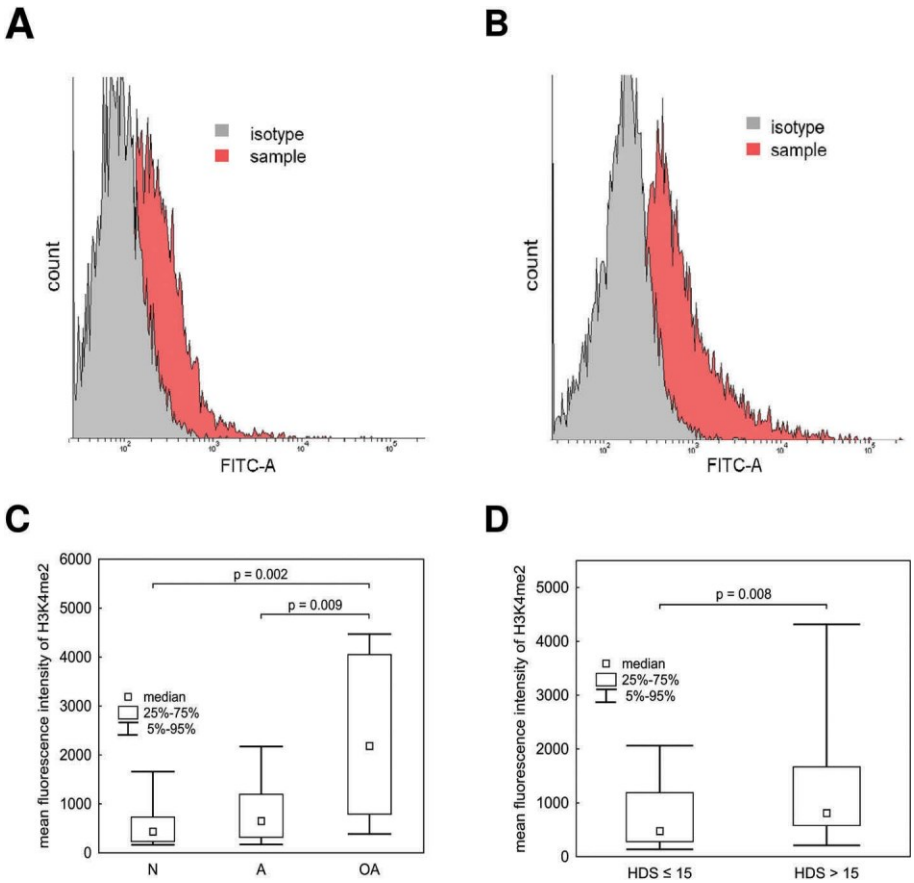

Figure 2. Relationship between H3K4me2 labeling and semen quality or chromatin maturity. A) Representative images of H3K4me2 histograms generated by flow cytometry, including a normospermic sample with HDS ≤ 15; B) and a sample with pathological semen quality and HDS > 15. C) Comparison of H3K4me2 fluorescence intensity between normozoospermic (N), asthenozoospermic (A), and oligoasthenozoospermic (OA) samples; D) and between samples with HDS ≤ 15 and HDS > 15. The data are expressed as medians and appropriate quartiles, and different superscripts indicate statistical significance ($p < 0.05$). HDS, high DNA stainability index; DFI, DNA fragmentation index.

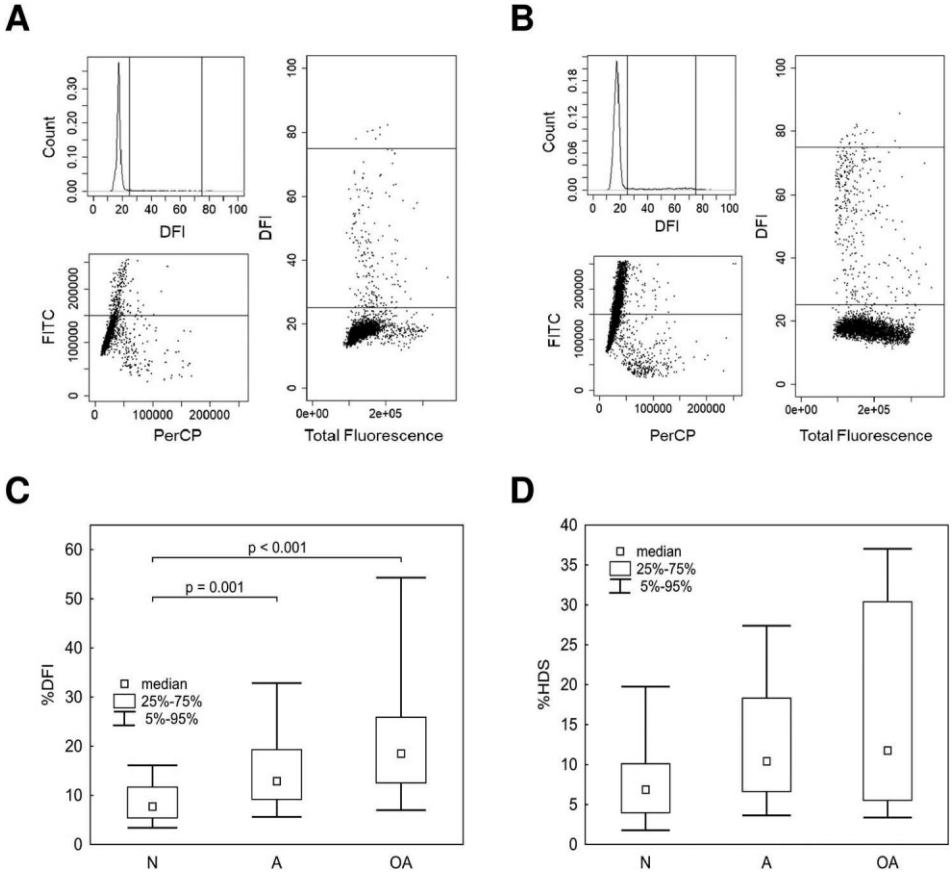

Figure 3. Relationship between semen quality and DNA fragmentation or chromatin maturity measured by SCSA. A) Representative histograms and scatter diagrams of the SCSA results for samples with HDS ≤ 15; B) and HDS > 15; C) Comparison of %DFI; D) and % HDS between normozoospermic (N), asthenozoospermic (A), and oligoasthenozoospermic (OA) samples. The data are expressed as medians and appropriate quartiles, and different superscripts indicate statistical significance ($p < 0.05$). HDS, high DNA stainability index; DFI, DNA fragmentation index.

2012). This suggests that, H3K4me2 may be a better indicator than %HDS.

Previous studies have shown that incomplete protamination, the protamine ratio, and PTMs of residual histones are reliable prognostic markers for ART success and embryo quality (Carrell et al. 1999; Aoki et al. 2005; Nasr-Esfahani et al. 2007; de Mateo et al. 2009; Simon et al. 2011). We performed the first comparative analysis of variation in H3K4me2 among semen samples classified by pathological semen quality. H3K4me2 reflects sperm histone code quality as well as protamine features and is advanta- geous for the assessment of sperm. H3K4me2 levels can partially reflect persisting H3 histones and a shift in the protamine-histone ratio in incompletely prota- minated sperm heads (Hamad et al. 2014) but the distribution of H3K4me2 did not show an identical pattern to that of H3 in sperm heads (van der Heijden et al. 2008). Moreover, our investigation did not reveal strict dependency of the H3K4me2 level to total his- tone H3 (own unpublished data).

In general, deviations in the sperm histone code have been associated with sperm incompetency and decreased fertility (Gunes et al. 2016; Kutchy et al. 2017; Rogenhofer et al. 2017; Schon et al. 2019). The heritability (Jenkins and Carrell 2011; Aoshima et al. 2015; Colaco and Sakkas 2018) of sperm epigenetic marks emphasizes the significance of the H3K4me2 label as an marker of sperm quality. Further studies of the sperm epigenome can improve our understanding of sperm function, explain cases of idiopathic infertility, and improve sperm selection for ART protocols (Castillo et al. 2011; Siklenka et al. 2015; Gunes et al. 2016; Bracke et al. 2018). For routine usage, studies of epigenetic marks, selectable sperm labels, and appropriate combinations with noninvasive sperm selection approaches are needed (Ozanon et al. 2005; Štiavnická et al. 2017). Thus, we expect H3K4me2 may become part of a sperm quality indicator together with pre- viously established noninvasive methods for sperm selection, such as SUTI (sperm ubiquitin tag assay) or MACS (magnetic-activated cell sorting) (Ozanon et al.

2005; Nasr-Esfahani et al. 2012). Moreover, Raman spectroscopy has potential as a noninvasive method for sperm selection with the ability to distinguish epi- genetic differences (Poplineau et al. 2011).

By combining three different methods of evaluation, the study supports H3K4me2 as an indicator of aberrant histone-protamine exchange, resulting in improper chromatin condensation. This would also be reflected in the distribution and amount of residual histones and PTMs. Thus, the impact of H3K4me2 on ART success should be assessed as compared to the intragenomic H3K4me2 distribution among spermatozoa with different grades of chromatin maturity.

Materials and methods

Materials

Chemicals were purchased from Sigma-Aldrich (St. Louis, MO, USA), unless otherwise stated.

Sperm samples

Human ejaculate samples were obtained after obtaining written consent at the ART center Genetika Pilsen Ltd. (Pilsen, Czech Republic). All subjects were strictly anonymous to the research team. The study was approved by the Ethics committee of Charles University, Faculty of Medicine in Pilsen (238/2016).

Twenty-two sperm samples from healthy donors (normozoospermic, N) and 77 samples from men with pathological semen quality, including 63 present- ing with asthenozoospermia (A; progressive motility below 32%) and 14 with oligoasthenozoospermia (OA, concentration below 15 mil/ml and progressive motility under 32%), were assessed. The evaluations of semen concentration, motility, and classification according semen quality were performed in compliance with WHO standards (2010).

Mitochondrial membrane potential and early apoptotic spermatozoa

For the detection of mitochondrial activity and early apoptosis, sperm samples were incubated with 100 nM MitoTracker Deep Red (Thermo Fisher Scientific, Waltham, MA, USA) and 50 nM YO-PRO1 (Thermo Fisher Scientific) in Biggers-Whitten Whittingham medium (BWW) (Biggers et al. 1971) for 30 min at room temperature in the dark. Acquisition was per- formed using a FACSVerse Flow Cytometer (Becton Dickinson, San Diego, CA, USA) containing BD FACSuite software (Becton Dickinson). Cells were run through the instrument at 150 to 300 cells/s and data were collected from 5000 cells. Excitation was performed with a 488-nm laser, except for MitoTracker Deep Red, which was excited at 640 nm. YO-PRO1 green fluorescence was detected with a 537/ 32BP filter and MitoTracker Deep Red was detected with a 586/42BP filter. MitoTracker+/YO-PRO1- spermatozoa were considered viable with active mitochondria, and MitoTracker-/YO-PRO1+ were identified as early apoptotic spermatozoa with non-functional mitochondria. Flow cytometry data were analyzed using WEASEL Ver. 3 (WEHI, Melbourne, Australia).

Sperm chromatin structure assay (SCSA)

A sperm chromatin structure assay was performed according to the protocol described by Evenson and Jost (2000). This technique is based on the vulnerability of sperm DNA to acid-induced denaturation *in situ* and subsequent metachromatic staining with acridine orange (AO). The DNA fragmentation index (%DFI) and high DNA stainability (%HDS), indicators of chromatin immaturity (i.e., protamination completeness), were assessed. The samples were evaluated using the FACSVerse Flow Cytometer controlled with BD FACSuite. Data were collected from 5000 events. Excitation of acridine orange was performed with a blue laser (488 nm); red fluorescence was detected with a 700/ 54BP filter and green fluorescence was detected with a 537/32BP filter. Each sample was run twice and data were analyzed using WEASEL Ver. 3 (WEHI).

Western blot analysis of H3K4me2

Based on the SCSA results, samples with %HDS ≤ 15 and % HDS > 15 (Evenson 2011) were compared with respect to H3K4me2 levels by western blotting. Samples were washed twice with PBS and subsequently dissolved in lysis buffer (7 M urea, 2 M thiourea, 4% CHAPS, 120 mM DTT, 40 mM TRIS base) for 30 min on ice. Pooled samples from five patients were prepared and solubilized with the Laemmli buffer (0.003% Triton-X-100 and 0.001% SDS), enriched with Complete Mini Protease Inhibitor Cocktail (Roche, Basel, Switzerland). Thereafter, samples were boiled and subjected to SDS-PAGE on 12.5% separating gels and blotted using the Trans-Blot Turbo Transfer System (BioRad Laboratories, Steenvoorde, France) onto a PVDF membrane (GE Healthcare Life Sciences, Amersham, UK). Approximately 10 million spermatozoa were loaded for each line. Then, the membrane was blocked in 1% BSA in TBS with 0.5% Tween-20 (TBS-T) for 60 min at room temperature. H3K4me2 was detected by rabbit polyclonal anti-H3K4me2 (1:1.000, Abcam, Cambridge, UK), overnight at 4°C. Mouse polyclonal antibody against α-tubulin was used as a loading control (1:1.000, Sigma-Aldrich). Horseradish peroxidase (HRP)-conjugated secondary antibodies, goat anti-mouse, or anti-

rabbit IgG (1:15.000; Invitrogen, Waltham, MA, USA), were applied. Target proteins were visualized using ECL Select Western Blotting Detection Reagent (GE Healthcare Life Sciences, Amersham, UK) and the ChemiDoc MP System (Bio-Rad). Densitometry analysis was performed using Image Lab 6.0.1 software (Biorad).

Immunolocalization of H3K4me2

Sperm samples were washed with PBS, placed on microscope slides, and allowed to dry. The spermatozoa on the slides were fixed with 4% paraformaldehyde for 15 min and washed with PBS. They were then permeabilized with 0.5% Triton X-100 and blocked with a solution of 5% normal goat serum (NGS) and 0.1% TritonX-100 in PBS for 60 min at room temperature. Subsequently, the spermatozoa were incubated with a rabbit polyclonal anti-H3K4me2 antibody (1:100; Abcam) for 60 min at room temperature, washed twice with PBS, and incubated with AlexaFluor 488-conjugated goat anti-rabbit secondary antibody (1:200). For negative controls, non-immune rabbit serum with comparable globulin concentrations was used instead of primary antibodies and processed in the same way. Finally, sperm samples were washed twice and mounted onto slides in VectaShield medium with 4′6′-diamidino-2-phenylindole (DAPI; Vector Laboratories Inc., Burlingame, CA, USA). Images were acquired using a 125 spinning disk confocal microscope, Olympus IX83 (Dusseldorf, Germany) and VisiView® (Visitron Systems GmbH, Puchheim, Germany).

H3K4me2 detection by flow cytometry

For H3K4me2 detection, sample preparation and histone analysis by flow cytometry were performed according to the methods of Li et al. (2006). For the detection of H3K4me2, a polyclonal rabbit anti-H3K4me2 antibody (1:100) and Alexa Fluor 488-conjugated goat anti-rabbit secondary antibody (1:200; Abcam) were used. Acquisition was performed using the FACSVerse Flow Cytometer and BD FACSuite. Data were collected from 5000 events. A blue laser (488 nm) was used and fluorescence signals were collected using the 537/32BP filter for the excitation of Alexa Fluor 488. An isotype control was evaluated for each sample, and mean fluorescence intensity was measured using the sample and isotype control. Data were analyzed using WEASEL Ver. 3 (WEHI), and the final value for H3K4me2 fluorescence intensity was obtained after subtracting the mean fluorescence intensity of the isotype control from the signal of the sample.

Statistical analysis

Data from all analyses are expressed as the medians with appropriate quantiles and were processed using Statistica Cz 12 (StatSoft, Tulsa, OK, USA). Data were significantly non-normally distributed (according to Shapiro-Wilk tests); accordingly, nonparametric methods were used. Kruskal–Wallis ANOVA (for quantitative variables) was applied for the comparison of all parameters between patient groups with different semen quality. In the case of significant overall findings, pairwise differences between groups were assessed by post-hoc multiple com- parisons of mean ranks according to Siegel and Castellan (1988), Mann–Whitney U tests, and a Bonferroni adjust- ment for multiple testing.

In addition, selected parameters were subjected to Spearman's rank correlation test. The level of statistical significance was set to $p < 0.05$, and two-tailed p-values are indicated.

Acknowledgments

We would like to thank Ms. Kathryn Craighead for manuscript editing. This work was supported by the Czech Health Research Council (NV18-01-00544), Charles University Research Fund (PROGRES Q39), the National Sustainability Programme I (NPU I) Nr LO1503 provided by the Ministry of Education, Youth and Sports of the Czech Republic (MEYS CR), project no. SVV 02690 provided by MEYS CR, and project no. CZ.02.1.01/0.0/0.0/16_019/0000787 "Fighting Infectious Diseases" awarded by MEYS CR and financed by The European Regional Development Fund. O.GA. was supported by the University of Castilla-La Mancha and Junta de Comunidades de Castilla-La Mancha (SBPLY/17/180501/000470). P.S. was supported by seed funding from the F21C program of the University of Missouri.

Disclosure statement

No potential conflict of interest was reported by the authors.

Funding

This work was supported by the University of Castilla-La Mancha and Junta de Comunidades de Castilla-La Mancha [SBPLY/17/180501/000470]; National Sustainability Programme I provided by the Ministry of Education, Youth and Sports of the Czech Republic [Nr. LO1503]; Ministry of Education, Youth and Sports of the Czech Republic [No. SVV 02690]; Charles University Research Fund [PROGRES Q39]; Ministry of Education, Youth and Sports of the Czech Republic and financed from The European Regional Development Fund [No. CZ.02.1.01/0.0/0.0/16_019/0000787 "Fighting]; University of Missouri [F21C program].

Authors' contributions

Participated in study design, experiments and manuscript preparation: MŠ, OGA, JN; Participated in experiments: LAP, MD, MK, JM, HŘ, LG, TF; Co-wrote the manuscript and participated in experimental design: PS; Analyzed data:

PH; Provided human samples and key information: ZUG, PL (from the Center of Assisted Reproduction Genetika Pilsen Ltd., Pilsen, Czech Republic); Supervised the collaboration with Genetika Ltd. and participated in manuscript preparation: MK.

References

Aoki VW, Liu L, Carrell DT. 2005. Identification and evaluation of a novel sperm protamine abnormality in a population of infertile males. Hum Reprod. 20:1298–1306. doi:10.1093/humrep/deh798

Aoshima K, Inoue E, Sawa H, Okada Y. 2015. Paternal H3K4 methylation is required for minor zygotic gene activation and early mouse embryonic development. EMBO Rep. 16:803–812.

Bahreinian M, Tavalaee M, Abbasi H, Kiani-Esfahani A, Shiravi AH, Nasr-Esfahani MH. 2015. DNA hypomethylation predisposes sperm to DNA damage in individuals with varicocele. Syst Biol Reprod Med. 61:179–186. doi:10.3109/19396368.2015.1020116

Balhorn R. 2007. The protamine family of sperm nuclear proteins. Genome Biol. 8:227. doi:10.1186/gb-2007- 8-9-227

Biggers JD, Whitten WK, Whittingham DG. 1971. The culture of mouse embryos in vitro. In *Methods in Mammalian Embryology* (ed. JC Daniels, Jr.). San Francisco: Freeman; p. 86–116.

Bracke A, Peeters K, Punjabi U, Hoogewijs D, Dewilde S. 2018. A search for molecular mechanisms underlying male idiopathic infertility. Reprod Biomed Online. 36:327–339.

Brykczynska U, Hisano M, Erkek S, Ramos L, Oakeley EJ, Roloff TC, Beisel C, Schübeler D, Stadler MB, Peters AHFM. 2010. Repressive and active histone methylation mark distinct promoters in human and mouse spermatozoa. Nat Struct Mol Biol. 17:679–687. doi:10.1038/nsmb.1821

Carrell DT, Emery BR, Hammoud S. 2007. Altered protamine expression and diminished spermatogenesis: what is the link? Hum Reprod Update. 13:313–327. doi:10.1093/humupd/dml057

Carrell DT, Emery BR, Liu L. 1999. Characterization of aneuploidy rates, protamine levels, ultrastructure, and functional ability of round-headed sperm from two sib- lings and implications for intracytoplasmic sperm injection. Fertil Steril. 71:511–516.

Castillo J, Simon L, de Mateo S, Lewis S, Oliva R. 2011. Protamine/DNA ratios and DNA damage in native and density gradient centrifuged sperm from infertile patients. J Androl. 32:324–332. doi:10.2164/jandrol.110.011015

Colaco S, Sakkas D. 2018. Paternal factors contributing to embryo quality. J Assist Reprod Genet. 35:1953–1968. doi:10.1007/s10815-018-1304-4

de Mateo S, Gázquez C, Guimerà M, Balasch J, Meistrich ML, Ballescà JL, Oliva R. 2009. Protamine 2 precursors (Pre-P2), protamine 1 to protamine 2 ratio (P1/P2), and assisted reproduction outcome. Fertil Steril. 91:715–722. doi:10.1016/j.fertnstert.2007.12.047

Delbes G, Hales BF, Robaire B. 2010. Toxicants and human sperm chromatin integrity. Mol Hum Reprod. 16:14–22. doi:10.1093/molehr/gap087

Eelaminejad Z, Favaedi R, Sodeifi N, Sadighi Gilani MA, Shahhoseini M. 2017. Deficient expression of JMJD1A histone demethylase in patients with round spermatid maturation arrest. Reprod Biomed Online. 34:82–89.

Elshal MF, El-Sayed IH, Elsaied MA, El-Masry SA, Kumosani TA. 2009. Sperm head defects and disturbances in spermatozoal chromatin and DNA integrities in idio- pathic infertile subjects: association with cigarette smoking. Clin Biochem. 42:589–594. doi:10.1016/j.clinbiochem.2008.11.012

Evenson D, Jost L. 2000. Sperm chromatin structure assay is useful for fertility assessment. Methods Cell Sci. 22:169–189.

Evenson DP. 2011. Sperm chromatin structure assay (SCSA®): 30 years of experience with the SCSA®. Sperm Chromatin. Springer New York, New York, NY:125–149. doi:10.1007/978-1-4419-6857-9_9

Godmann M, Auger V, Ferraroni-Aguiar V, Di Sauro A, Sette C, Behr R, Kimmins S. 2007. Dynamic regulation of histone H3 methylation at lysine 4 in mammalian spermatogenesis. Biol Reprod. 77:754–764. doi:10.1095/biolreprod.107.062265

Gunes S, Arslan MA, Hekim GNT, Asci R. 2016. The role of epigenetics in idiopathic male infertility. J Assist Reprod Genet. 33:553–569. doi:10.1007/s10815-016-0682-8

Gunes S, Metin Mahmutoglu A, Arslan MA, Henkel R. 2018. Smoking-induced genetic and epigenetic alterations in infertile men. Andrologia. 50:e13124.

Hamad MF, Shelko N, Kartarius S, Montenarh M, Hammadeh ME. 2014. Impact of cigarette smoking on his- tone (H2B) to protamine ratio in human spermatozoa and its relation to sperm parameters. Andrology. 2:666–677.

Hammoud SS, Nix DA, Hammoud AO, Gibson M, Cairns BR, Carrell DT. 2011. Genome-wide analysis iden- tifies changes in histone retention and epigenetic modifi- cations at developmental and imprinted gene loci in the sperm of infertile men. Hum Reprod. 26:2558–2569. doi:10.1093/humrep/der192

Hammoud SS, Nix DA, Zhang H, Purwar J, Carrell DT, Cairns BR. 2009. Distinctive chromatin in human sperm packages genes for embryo development. Nature. 460:473–478.

Jenkins TG, Carrell DT. 2011. The paternal epigenome and embryogenesis: poising mechanisms for development. Asian J Androl. 13:76–80.

Jenkins TG, James ER, Alonso DF, Hoidal JR, Murphy PJ, Hotaling JM, Cairns BR, Carrell DT, Aston KI. 2017. Cigarette smoking significantly alters sperm DNA methylation patterns. Andrology. 5:1089–1099. doi:10.1111/andr.12416

Kiani-Esfahani A, Bahrami S, Tavalaee M, Deemeh MR, Mahjour AA, Nasr-Esfahani MH. 2013. Cytosolic and mitochondrial ROS: which one is associated with poor chromatin remodeling? Syst. Biol Reprod Med. 59:352–359. doi:10.3109/19396368.2013.829536

Kutchy NA, Menezes ESB, Chiappetta A, Tan W, Wills RW, Kaya A, Topper E, Moura AA, Perkins AD, Memili E. 2017. Acetylation and methylation of sperm histone 3 lysine 27 (H3K27ac and H3K27me3) are associated with bull fertility. Andrologia. e12915. doi:10.1111/and.12915

La Spina FA, Romanato M, Brugo-Olmedo S, De Vincentiis S, Julianelli V, Rivera RM, Buffone MG. 2014. Heterogeneous distribution of histone methylation in mature human sperm. J Assist Reprod Genet. 31:45–49.

Li Z, Yang J, Huang H. 2006. Oxidative stress induces H2AX phosphorylation in human spermatozoa. FEBS Lett. 580:6161–6168. doi:10.1016/j.febslet.2006.10.016

Luense LJ, Wang X, Schon SB, Weller AH, Lin Shiao E, Bryant JM, Bartolomei MS, Coutifaris C, Garcia BA, Berger SL. 2016. Comprehensive analysis of histone post-translational modifications in mouse and human male germ cells. Epigenetics Chromatin. 9:24. doi:10.1186/s13072-016-0072-6

Maselli J, Hales BF, Chan P, Robaire B. 2012. Exposure to bleomycin, etoposide, and Cis-platinum alters rat sperm chromatin integrity and sperm head protein Profile1. Biol Reprod. 86. doi:10.1095/biolreprod.111.098616.

Nasr-Esfahani MH, Deemeh MR, Tavalaee M. 2012. New era in sperm selection for ICSI. Int J Androl. 35:475–484. doi:10.1111/j.1365-2605.2011.01227.x

Nasr-Esfahani MH, Razavi S, Mardani M, Shirazi R, Javanmardi S. 2007. Effects of failed oocyte activation and sperm protamine deficiency on fertilization post-ICSI. Reprod Biomed Online. 14:422–429.

Nevoral J, Sutovsky P. 2017. Epigenome modification and ubiquitin-dependent proteolysis during pronuclear development of the mammalian zygote: animal models to study pronuclear development. Animal Models and Human Reproduction. New Jersey: Wiley Blackwell; p. 435–466. doi:10.1002/9781118881286.ch17.

Oliva R. 2006. Protamines and male infertility. Hum Reprod Update. 12:417–435. doi:10.1093/humupd/dml009

Ozanon C, Chouteau J, Sutovsky P. 2005. Clinical adaptation of the sperm ubuquitin tag immunoassay (SUTI): relationship of sperm ubiquitylation with sperm quality in gradient-purified semen samples from 93 men from a general infertility clinic population. Hum Reprod. 20:2271–2278. doi:10.1093/humrep/dei013

Pérez-Cerezales S, Ramos-Ibeas P, Lopez-Cardona A, Pericuesta E, Fernandez-Gonzalez R, Pintado B, Gutierrez-Adan A. 2017. Elimination of methylation marks at lysines 4 and 9 of histone 3 (H3K4 and H3K9) of spermatozoa alters offspring phenotype. Reprod Fertil Dev. 29:740. doi:10.1071/RD15349

Poplineau M, Trussardi-Régnier A, Happillon T, Dufer J, Manfait M, Bernard P, Piot O, Antonicelli F. 2011. Raman microspectroscopy detects epigenetic modifications in living Jurkat leukemic cells. Epigenomics. 3:785–794.

Rathke C, Baarends WM, Awe S, Renkawitz-Pohl R. 2014. Chromatin dynamics during spermiogenesis. Biochim Biophys Acta - Gene Regul Mech. 1839:155–168. doi:10.1016/j.bbagrm.2013.08.004

Rathke C, Baarends WM, Jayaramaiah-Raja S, Bartkuhn M, Renkawitz R, Renkawitz-Pohl R. 2007. Transition from a nucleosome-based to a protamine-based chromatin configuration during spermiogenesis in Drosophila. J Cell Sci. 120:1689–1700. doi:10.1242/jcs.004663

Rogenhofer N, Ott J, Pilatz A, Wolf J, Thaler CJ, Windischbauer L, Schagdarsurengin U, Steger K, von Schönfeldt V. 2017. Unexplained recurrent miscarriages are associated with an aberrant sperm protamine mRNA content. Hum Reprod. 32:1574–1582. doi:10.1093/humrep/dex224

Schon SB, Luense LJ, Wang X, Bartolomei MS, Coutifaris C, Garcia BA, Berger SL. 2019. Histone modification signatures in human sperm distinguish clinical abnormalities. J Assist Reprod Genet. 36:267–275.

Sharma U, Sun F, Conine CC, Reichholf B, Kukreja S, Herzog VA, Ameres SL, Rando OJ. 2018. Small RNAs are trafficked from the epididymis to developing mammalian sperm. Dev Cell. 46:481–494.e6. doi:10.1016/j.devcel.2018.06.023

Siegel S, Castellan NJ. 1988. Non-parametric statistics for the behavioural sciences. New York: MacGraw Hill Int. doi:10.1007/s00464-002-9121-2

Siklenka K, Erkek S, Godmann M, Lambrot R, McGraw S, Lafleur C, Cohen T, Xia J, Suderman M, Hallett M, et al. 2015. Disruption of histone methylation in developing sperm impairs offspring health transgenerationally. Science. 350:aab2006. doi:10.1126/science.aab2006

Simon L, Castillo J, Oliva R, Lewis SEM. 2011. Relationships between human sperm protamines, DNA damage and assisted reproduction outcomes. Reprod Biomed Online. 23:724–734. doi:10.1016/j.rbmo.2011.08.010

Speyer BE, Pizzey AR, Abramov B, Saab W, Doshi A, Sarna U, Harper JC, Serhal P. 2015. Successful outcomes achieved in assisted reproduction cycles using sperm with high levels of high DNA stainability. Syst Biol Reprod Med. 61:293–299. doi:10.3109/19396368.2015.1033065

Štiavnická M, Abril-Parreño L, Nevoral J, Králíčková M, García-Álvarez O. 2017. Non-invasive approaches to epigenetic-based sperm selection. Med Sci Monit. 23:4677–4683.

Talebi AR, Moein MR, Tabibnejad N, Ghasemzadeh J. 2008. Effect of varicocele on chromatin condensation and DNA integrity of ejaculated spermatozoa using cytochemical tests. Andrologia. 40:245–251.

Tavalaee M, Razavi S, Nasr-Esfahani MH. 2009. Influence of sperm chromatin anomalies on assisted reproductive technology outcome. Fertil Steril. 91:1119–1126. doi:10.1016/j.fertnstert.2008.01.063

Teperek M, Simeone A, Gaggioli V, Miyamoto K, Allen GE, Erkek S, Kwon T, Marcotte EM, Zegerman P, Bradshaw CR, et al. 2016. Sperm is epigenetically pro- grammed to regulate gene transcription in embryos. Genome Res. 26:1034–1046. doi:10.1101/gr.201541.115

Tunc O, Tremellen K. 2009. Oxidative DNA damage impairs global sperm DNA methylation in infertile men. J Assist Reprod Genet. 26:537–544.

van der Heijden GW, Derijck AAHA, Ramos L, Giele M, van der Vlag J, de Boer P. 2006. Transmission of modified nucleosomes from the mouse male germline to the zygote and subsequent remodeling of paternal chromatin. Dev Biol. 298:458–469. doi:10.1016/j.ydbio.2006.06.051

van der Heijden GW, Ramos L, Baart EB, van Den Berg IM, Derijck AA, van der Vlag J, Martini E, de Boer P. 2008. Sperm-derived histones contribute to zygotic chromatin in humans. BMC Dev Biol. 8:34.

World Health Organization. 2010. WHO laboratory manual for the examination and processing of human semen. Geneva: World Health Organization.

Yeung CH, Beiglböck-Karau L, Tüttelmann F, Nieschlag E. 2007. The presence of germ cells in the semen of azoospermic, cryptozoospermic and severe oligozoospermic patients: stringent flow cytometric analysis and correlations with hormonal status. Clin Endocrinol. 67:767–775.

Zhong HZ, Lv FT, Deng XL, Hu Y, Xie DN, Lin B, Mo ZN, Lin FQ. 2015. Evaluating γH2AX in spermatozoa from male infertility patients. Fertil Steril. 104:574–581. doi:10.1016/j.fertnstert.2015.06.004

A2

Řimnáčová H., Štiavnická M., Moravec J., Chemek M., Kolinko Y., García-Álvarez O., Mouton P.R., Trejo A.M.C., Fenclová T., Eretová N., Hošek P., Klein P., Králíčková M., Petr J., Nevoral J. 2020. Low doses of Bisphenol S affect post-translational modifications of sperm proteins in male mice. Reprod Biol Endocrinol. 18(1):56. doi: 10.1186/s12958-020-00596-x. (**IF_{2020} = 5.211**)

Řimnáčová et al. Reproductive Biology and Endocrinology (2020) 18:56
https://doi.org/10.1186/s12958-020-00596-x

Reproductive Biology and Endocrinology

RESEARCH Open Access

Low doses of Bisphenol S affect post-translational modifications of sperm proteins in male mice

Hedvika Řimnáčová[1*†], Miriam Štiavnická[1†], Jiří Moravec[1], Marouane Chemek[1,2], Yaroslav Kolinko[1,3], Olga García-Álvarez[1,4], Peter R. Mouton[5], Azalia Mariel Carranza Trejo[1], Tereza Fenclová[1], Nikola Eretová[1], Petr Hošek[1], Pavel Klein[1], Milena Králíčková[1,3], Jaroslav Petr[6] and Jan Nevoral[1,3]

Abstract

Background: Bisphenol S (BPS) is increasingly used as a replacement for bisphenol A in the manufacture of products containing polycarbonates and epoxy resins. However, further studies of BPS exposure are needed for the assessment of health risks to humans. In this study we assessed the potential harmfulness of low-dose BPS on reproduction in male mice.

Methods: To simulate human exposure under experimental conditions, 8-week-old outbred ICR male mice received 8 weeks of drinking water containing a broad range of BPS doses [0.001, 1.0, or 100 μg/kg body weight (bw)/day, BPS1–3] or vehicle control. Mice were sacrificed and testicular tissue taken for histological analysis and protein identification by nano-liquid chromatography/mass spectrometry (MS) and sperm collected for immunodetection of acetylated lysine and phosphorylated tyrosine followed by protein characterisation using matrix-assisted laser desorption ionisation time-of-flight MS (MALDI-TOF MS).

Results: The results indicate that compared to vehicle, 100 μg/kg/day exposure (BPS3) leads to 1) significant histopathology in testicular tissue; and, 2) higher levels of the histone protein γH2AX, a reliable marker of DNA damage. There were fewer mature spermatozoa in the germ layer in the experimental group treated with 1 μg/kg bw (BPS2). Finally, western blot and MALDI-TOF MS studies showed significant alterations in the sperm acetylome and phosphorylome in mice treated with the lowest exposure (0.001 μg/kg/day; BPS1), although the dose is several times lower than what has been published so far.

Conclusions: In summary, this range of qualitative and quantitative findings in young male mice raise the possibility that very low doses of BPS may impair mammalian reproduction through epigenetic modifications of sperm proteins.

Keywords: Male reproduction, Endocrine disruptor, Low dose effect, Bisphenol S, Post-translational modification

* Correspondence: hedvika.rimnacova@lfp.cuni.cz
†Hedvika Řimnáčová and Miriam Štiavnická contributed equally to this work.
[1]Biomedical Center in Pilsen, Faculty of Medicine in Pilsen, Charles University, alej Svobody 1655/76, Pilsen, Czech Republic
Full list of author information is available at the end of the article

Introduction

Bisphenol A (BPA) is well-documented as an endocrine disruptor with detrimental effects on reproduction [1]; as a result of increasing scrutiny of BPA, there is a broad interest in substitution of alternative bisphenols for human consumption. The most common alternative bisphenol, Bisphenol S (BPS), includes a sulfone group (SO_2) in place of the dimethylmethylene group [C $(CH3)_2$] in BPA [2]. BPS has shown a range of deleteri- ous effects following oral ingestion, inhalation or dermal absorption [3], with the most common route of intake for humans being exposure through contaminated water and food at relatively low doses [4]. To date, however, there have been only limited experimental studies of the possible harmfulness of low BPS doses.

Previous studies of BPS in male rats have reported a range of deleterious effects on hormonal balance, reduced germinal epithelium of seminiferous tubules and increased generation of reactive oxygen species [5, 6]. Recent studies have reported BPS induces epigenetic changes, including alterations in the histone code in oocytes, increased DNA methylation in mouse spermatocytes and changes to transcriptome and proteome of cells in testicular tissue and many other cells types [7–10]. Collectively, these findings suggest BPS may disrupt male reproductive functions through post-translational modifications (PTMs) of nucleic acids and proteins [1, 11, 12] and regulation of transcriptionally silenced spermatozoa [13]. In particular, lysine acetylation and tyrosine phosphorylation of sperm proteins regulate spermatogenesis and sperm capacitation [14–16]. Based on these studies, it is possible that low doses of BPS could modulate male reproduction through PTMs of protein and nucleic acid structure. BPS is classified as an endocrine disruptor and its dose-response is more likely to be nonmonotonic, hence, very-low doses may be more effective than high doses. Therefore, we have chosen wide range of much lower BPS doses than was published before [5, 6]. Using a wide range of low- and very-low doses BPS administered in drinking water for 8 weeks to young adult male mice, we want to determine the effect of BPS doses form the environment. Our find- ings provide one of the first indications that low doses of BPS regulate PTMs of spermatozoa and lead to possible negative effects on male reproduction.

Material and methods

All chemicals, including BPS (CAS: 80–09-1, cat. No. 103039) were purchased from Sigma-Aldrich (USA), unless stated otherwise.

Animals

All animal procedures were done in accordance with the Protection of Animals against Cruelty (Act No. 246/ 1992) under the supervision of the Animal Welfare Advisory Committee at the Ministry of Education, Youth, and Sports of the Czech Republic. Adult 7-week-old ICR male mice were purchased from Velaz Ltd. (Prague, Czech Republic), housed in standard cages in groups of 3 and maintained in a 12/12-h light/dark cycle at 21 ± 1 °C with a relative humidity of 60%. Bisphenol contamination was reduced using intact polysulfonate cages and glass drinking bottles. Mice were maintained on a phytoestrogen-free diet (1814P Altromin, Altromin Specialfutter GmbH & Co., Germany) with ultrapure water available ad libitum.

BPS dosage and sample collection

Mice were randomized into four experimental groups and allowed to adapt for 1 week. Vehicle control (0.1% ethanol; VC) and BPS for three treatment groups were administered through drinking water at final concentra- tions of 0, 0.0038, 3.8, and 380 μg/L, respectively, for 8 weeks (8–16 weeks of age). The following dosages were presumed [0, 0.001, 1, and 100 μg/kg body weight (bw)/ day] with actual exposure estimated based on the know- ledge of recorded body weight and water intake as previ- ously reported [17]. A wide range of doses and the route of exposure have been chosen appropriate to the real human exposure; doses of experimental animals through the drinking water have been used with respect to the welfare of animals. Hereafter, experimental groups will be stated as BPS1, BPS2 and BPS3.

Nine mice per group were included in three individual independent experiments (n = 36). Animal weights were recorded at the end of the experiments mice euthanised by cervical dislocation. Blood samples were collected by cardiac puncture, and serum was stored at − 80 °C until hormonal assay performance. Left and right testes were collected, weighed, and processed for histology and proteomics, respectively.

Sperm isolation and assessment

From the mice described above, the cauda epididymidis was dissected in 0.5 mL Whitten's medium (Suppl. Table S1), and sperm were allowed to swim out for 30 min. Thereafter, sperm concentration and motility were evaluated using Makler chamber and light microscope (Olympus CKX 41; Germany) equipped with a 10× objective (CAchN NA 0.25). 10 μl of sperm suspension was pipette to the Makler chamber, thereafter spermatozoa were counted in 3 lines, each of 10 squares and divide by 3 to obtain average sperm concentration in million per milliliter. Simul- taneously, each spermatozoon across the counted area was identified either as motile or immotile. Accord- ingly, the sperm motility was expressed as the ratio of motile to immotile spermatozoa. The analysis was performed blindly to avoid bias.

Hormonal profiling

Blood serum samples in three independent experiments (n = 5 mice per group) were assayed with Immunobeads Milliplex MAP kit (HPTP1MAG-66 K, MSHMAG-21 K; Merck Millipore, USA) for the following hormone levels: adrenocorticotropic hormone, follicle-stimulating hormone, growth hormone, luteinising hormone, thyroid-stimulating hormone, cortisol, progesterone, testosterone, triiodothyronine, and thyroxine.

Quantitative and qualitative analyses of testes

One testis from each animal (n = 9 per group) was fixed in Bouin solution, embedded in paraffin wax with random orientation, and sectioned completely into 10- μm-thick slides. The total testis volume, total germ epi- thelium volume, and interstitium volume were estimated according to the Cavalieri principle [18]. The fractions of spermatogenesis (pre-spermiation stages I–VI; middle spermiation stages VII–VIII; post-spermiation stages IX–XII) were found using the point grid approach [19, 20]. To determine the precision and accuracy of the stereological analysis, the coefficient of error was estimated (Suppl. Tab. S2) [18]. Qualitative analysis of seminiferous tubes was performed according to the methods described by the Society of Toxicologic Pathology [21, 22] to assess the following abnormalities: missing germ cell layers and germ cell depletion, retained spermatids (spermiation failure), multinucleate and apoptotic germ cells, and exfoliation of spermatogenic cells into the lumen. At least 100 seminiferous tubules were evaluated blind to treatment group for each testicular cross section. The quantitative assessment was performed on a Nikon Eclipse Ti-U microscope (Nikon, Japan) equipped with a motorised stage (Prior, UK) using a 10× objective (Plan Fluor, NA 0.3) and Stereologer 11 software (SRC, Biosciences Tampa, FL, USA) for histopathological evaluation was performed using a 40× objective (UPlanFl, NA 0.75).

Western blot

Testicular tissue and sperm were dissolved in lysis buffer (40 mM Tris base, 7 M urea, 2 M thiourea, 4% CHAPS, 120 mM dithiothreitol), enriched with Complete Mini Protease Inhibitor Cocktail (Roche, Switzerland), for 30 min on ice. Sperm samples of three individuals belong- ing to the same experimental group were pooled. There- after, samples were subjected to sodium dodecyl sulfate polyacrylamide gel electrophoresis on 4–15% separating Mini-PROTEAN precast gels and blotted using a Trans-Blot Turbo Transfer System onto polyvinylidene difluoride membranes (Bio-Rad Laboratories, France). The membranes were blocked in 1% bovine serum albumin in TBS with 0.5% Tween-20 for 60 min at room temperature and incubated overnight at 4 °C with primary antibodies diluted in blocking buffer. The following primary antibodies were used: anti-acetyl lysine antibodies (cat. no. ab80178; Abcam, UK), anti-phospho-tyrosine antibodies (cat. no. ab10321; Abcam), anti-acetylated α-tubulin antibodies, and anti-γH2AX antibodies. Mouse monoclonal anti-α-tubulin antibodies (cat. no. T6199; Sigma, St. Louis, MO, USA) and rabbit monoclonal anti-histone H3 antibodies (cat. no. D1H2; Cell Signaling Technology, Danvers, MA, USA) were used as the loading control for γH2AX and acetylated α-tubulin, respectively. Horseradish peroxidase-conjugated secondary antibodies (goat anti-mouse or anti-rabbit IgG; dilution: 1: 15,000; Invitrogen, Carlsbad, CA, USA) were applied for 60 min at 22 °C. Target proteins were visualised using ECL Select Western Blotting Detection Reagent (GE Healthcare Life Sciences, UK) and a ChemiDoc MP System (Bio-Rad). Alternatively, proteins were visua- lised using a colorimetric Opti-4CN substrate kit (Bio-Rad), followed by matrix-assisted laser desorption ionisation time-of-flight (MALDI-TOF) mass spectrometry (MS) for peptide detection in the dissected bands.

Proteome profiling

Testis lysates from animals in the experimental groups were collected for complete proteomic analysis. Nano-liquid chromatography-MS (nano-LC-MS) was used for protein identification and quantification, as described previously [7]. The acetylome and phosphorylome were analysed separately.

Statistics

The data were processed with GraphPad Prism 8 (GraphPad Software Inc., San Diego, CA, USA). Based on Shapiro-Wilk normality distribution tests, analysis of variance (ANOVA) and Kruskal-Wallis tests were used for normally and non-normally distributed data. In cases of significant overall findings, differences between indi- vidual group pairs were assessed by Tukey's and Dunn's post-hoc tests, respectively. Results with P less than 0.05 were considered statistically significant. Normally and non-normally distributed data were expressed as means and medians, respectively.

Results

Hormonal profiles and sperm features of BPS-treated males

At the end of 8-week exposure to actual doses of BPS, the body and testes weights were recorded and relative testes weights (mg/g bw) were determined. There were no differences between the experimental groups and the vehicle control (Table 1). Hormonal assays showed no significant differences in plasma hormone levels between the BPS-treated and vehicle control groups (Suppl. Table S3). Moreover, the spermatozoa

Table 1 Characteristics of experimental animals

	VC	BPS1	BPS2	BPS3
Weight of mouse body (g)	41,82 ± 0,72[a,b]	42,44 ± 0,77[a,b]	45,24 ± 1,36[a]	41,31 ± 1[b]
Relative weight of testes (mg/g of bw)	12,81 ± 0,30	12,76 ± 0,15	10,87 ± 0,37	11,03 ± 0,17

Body and relative testis weights are shown as means ± SEM of animals included in the study ($n = 9$ per experimental group). One-way ANOVA was followed by Tukey's multiple comparison tests. Different letters in the same row indicate significant differences ($p < 0.05$). *VC* vehicle control, *BPS1–3* increasing doses of bisphenol S

count was not affected by BPS exposure (Fig. 1a), although treatment with 0.001 μg/kg bw BPS1 decreased the portion of motile spermatozoa (Fig. 1b).

Higher BPS exposure induced abnormal testicular histopathology

Histological assessment was performed to evaluate the impact of actual BPS doses on testicular tissues. Stereological analysis showed no differences between groups in terms of testis volume, germinal epithelium volume (Fig. 2a, b), interstitium volume, germ layer volume fraction, and interstitium volume fraction. To investigate the effects of BPS treatments on spermatogenesis, individual stages of the seminiferous epithelium were identified and no differences between experimental groups were found (Fig. 2c, c'). Histopathological analysis of testicular tissues from BPS-exposed male mice showed an increased incidence of abnormalities in mice treated with the highest BPS dose (BPS3; Fig. 2d). In addition to vacuolisation of germ layer cells and enlarged multi-nuclear germ cells, the atypical residual bodies demonstrated the effects of BPS3 on testicular tissues (Fig. 2d–g). There were fewer mature spermatozoa in the germ layer in the BPS2 experimental group (Fig. 2h). Representative images of individual histopathologies are shown (Fig. 2d'–h').

Proteomic analysis of testicular tissue

Based on the different modes of action of BPS at various doses, whole-proteome profiling of testicular tissues was performed. In total, 3044 proteins were detected. Unique protein expression in the control and BPS-treated groups is shown in the Venn diagram in Fig. 3a. How- ever, after quantification of the levels of 1886 proteins, followed by subsequent principle component analysis (PCA), no distinct clusters of mice (n = 24) from individ- ual groups were observed, thus indicating a lack of a consistent proteome pattern (Fig. 3b). In addition to total protein analysis, acetylated (n = 15) and phosphory- lated (n = 26) peptides were quantified (Fig. 3c, d), and no significant differences were observed. Moreover, the deleterious effects of BPS3 were elucidated using anti- bodies against the phosphorylated form of H2AX (γH2AX) to label DNA double-stranded breaks; γH2AX is a representative PTM that can be used to identify DNA damage and cellular stress. Consistent with the increased incidence of abnormalities in seminiferous tubules in the BPS3 group, we observed an increase in the γH2AX signal as well (Fig. 3e).

Lower BPS exposure changed the post-translational quality of sperm proteins

In accordance with whole-proteome analysis of BPS-treated testes, analyses of the sperm acetylome and phosphorylome were performed using western blotting and MALDI-TOF MS. Because of the low protein amounts in sperm lysate extracts, sperm samples from three individuals belonging to the same experimental group were pooled, and three independent experiments

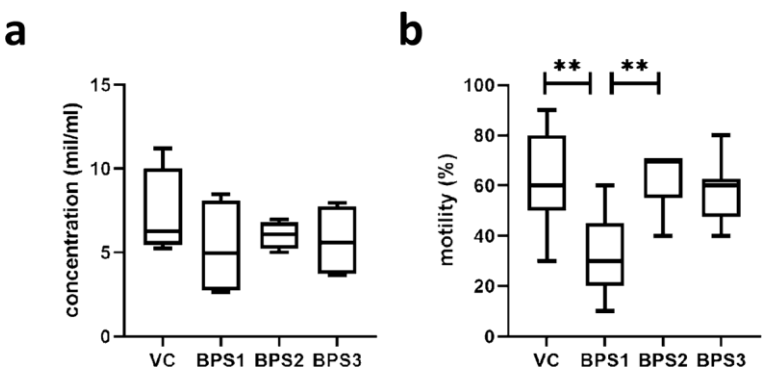

Fig. 1 Sperm features: (a) sperm concentration and (b) percentage of motile sperm. Data are shown as medians and 5–95% percentiles. Kruskal-Wallis tests followed by Dunn's multiple comparison tests were performed, and statistical significance is indicated (**$p < 0.01$). VC: vehicle control, BPS1–3: increasing doses of bisphenol S

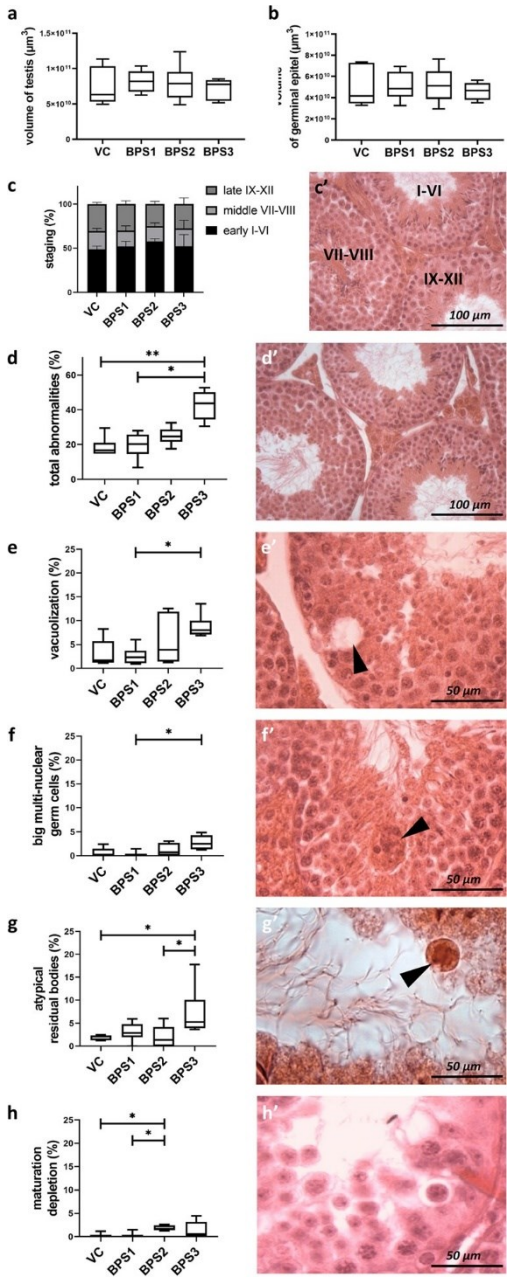

Fig. 2 Stereological and histopathological analyses of mouse testis in different treatment groups. (a) Fluctuations in the total testis volume (µm^3) in experimental groups; (b) volume of germinal epithelium (µm^3); and (c, c') stage of spermatogenesis (%) were recorded. Histopathological manifestations were tracked as follows: (d) portion of seminiferous tubule profiles containing an abnormality (%), including (e) tubes with vacuolisation (%), (f) tubes carrying large multinuclear germ cells (%), (g) atypical residual bodies (%), and/or (h) maturation depletion (%). (d') Representative images of healthy germ epithelium and (e'–h') individual abnormalities, respectively, are shown and indicated with arrowheads. Data are expressed as medians and 5–95% percentiles of six animals per experimental group. Kruskal-Wallis tests, followed by Dunn's multiple comparison tests, were performed, and statistical significance is indicated (*$p<0.05$, **$p<0.01$). VC: vehicle control, BPS1–3: increasing doses of bisphenol S

were performed. After loading equal amounts of protein per well, we found that the acetylation of proteins with molecular weights of approximately 37, 40, and 50 kDa were affected by treatment with BPS1 (Fig. 4a, b). Moreover, BPS1 also modified the phosphorylation of sperm proteins (37, 40, 85, and 100 kDa; Fig. 4c, d, d'). Candidate acetylated and phosphorylated proteins are summarised in Fig. 4 (e, f), and the results indicated the involvement of housekeeping proteins (ATP synthase subunit, hexokinase-1) and enzymes (DNA repair protein, E3 ubiquitin-protein ligase). In accordance with previous findings, demonstrating that BPS1 suppressed sperm motility, cytoskeletal factors (i.e., tubulin chains, actin; Fig. 4e) seems to be underwent to acetylation. Therefore, an antibody against acetylated α-tubulin (acTubulin) was used for a verification of tubulin as a candidate BPS target.

Next, we evaluated the densitometry of bands representing acetylated tubulin after treatment with BPS1 (Fig. 4g). Decreased tubulin acetylation was observed; however, the difference was not statistically significant, suggesting that other targets (such as ATP synthase and actin) may be related to sperm motility.

Discussion

Male reproduction involves sensitive machinery, which is required for spermatozoon development and can be affected by exposure to various environmental stimuli. Because mature spermatozoa have been transcriptionally silenced, changes in PTMs can regulate protein activity and modify other crucial biomolecules. Indeed, lysine acetylation and phosphorylation have been shown to be indispensable for the proper function of sperm [14, 15]. Our findings suggested that PTMs may be affected by pollutants from the environment. In our study, we simulated the exposure of adult males to BPS, a common endocrine disruptor, at very low doses (~ 0.001 and 1 µg/kg bw/day). Moreover, we chose ~ 100 µg/kg bw, which has been suggested to induce reproductive toxicity [3, 5]. The 8-week exposure covered the whole duration of spermatogenesis; therefore, we assumed that the sperm quality and testicular tissues would be affected at the tissue/cell and proteome levels. We also evaluated the effects of endocrine disruption on post-translational modifications of testicular/sperm proteins in accordance with our hypothesis of the "post-translational effect" of very low doses of these agents.

Recent studies have demonstrated that bisphenols alter steroid signalling pathways, having negative effects on male and female reproduction. Our observations did not reveal hormonal changes, even after higher BPS exposure, whereas comparable doses were found to be effect- ive in rats [6]. However, earlier results showing that endocrine disruptors lead to hormonal imbalances

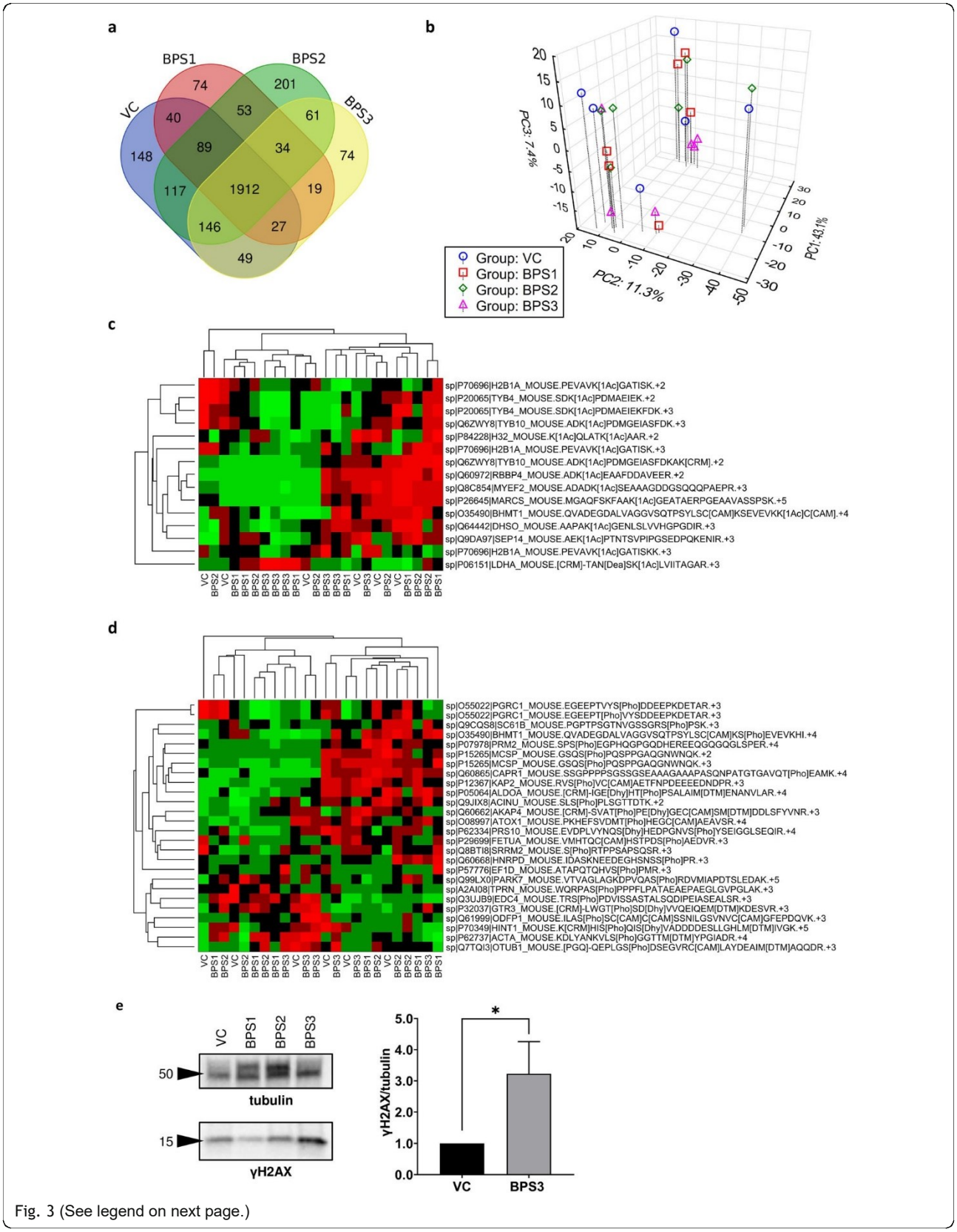

Fig. 3 (See legend on next page.)

(See figure on previous page.)
Fig. 3 Proteomic analysis of testicular tissues. (a) Venn diagram of total described testicular proteins in mice (n=4) after various treatments in different experimental groups. (b) Projection of 24 experimental mice into the space of first three principal components according to PCA; percentages in the axis legends show the proportion of total variance explained by the particular component. (c) Overview of acetylated and (d) phosphorylated testicular proteins. (e) Analysis of γH2AX; band signals were normalized to α-tubulin and related to the vehicle control as the mean (range) of three independent experiments. Unpaired t tests were performed, and statistical significance is indicated (*p<0.05). VC: vehicle control, BPS1–3: increasing doses of bisphenol S

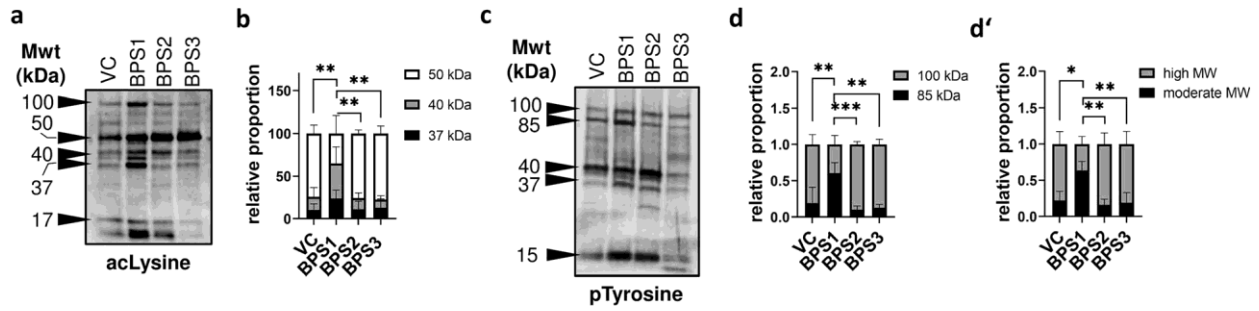

e

Band (~kDa)	unused	accession	protein
50	6.1	P56480	ATP synthase subunit beta, mitochondrial
	3.81	Q03265	ATP synthase subunit alpha, mitochondrial
	4	Q9D6F9	Tubulin beta-4A chain
	2.34	P05214	Tubulin alpha-3 chain
	2	P68134	Actin, alpha skeletal muscle
	2	Q5STT6	Protein FAM71B
40	2	P70388	DNA repair protein RAD50
	2	Q8BWR8	Rhophilin-2
37	2	Q61999	Outer dense fiber protein 1
	2	Q61127	NGFI-A-binding protein 2
	2	A7RDN6	Renalase
	2	A2ALU4	Protein Shroom2

f

Band (~kDa)	unused	accession	protein
100	6.05	P17710	Hexokinase-1
	4	O88987	A-kinase anchor protein 3
	2.03	Q60597	2-oxoglutarate dehydrogenase, mitochondrial
	2	P53566	CCAAT/enhancer-binding protein alpha
85	4	A3KGV1	Outer dense fiber protein 2
	2	Q80UP3	Diacylglycerol kinase zeta
	2	P70412	CUB and zona pellucida-like domain-containing protein 1
	2	Q925E0	Gamma-2-syntrophin
	2.13	P13020	Gelsolin
	2.04	Q9CU62	Structural maintenance of chromosomes protein 1A
	2	P53566	CCAAT/enhancer-binding protein alpha
	2	P35564	Calnexin
40	12.65	P63260	Actin, cytoplasmic 2
	4.06	P09041	Phosphoglycerate kinase 2
	2	Q7TPH6	E3 ubiquitin-protein ligase MYCBP2
	2	Q9CU62	Structural maintenance of chromosomes protein 1A
	2	Q9DB77	Cytochrome b-c1 complex subunit 2, mitochondrial
	2	Q9CZU6	Citrate synthase, mitochondrial
37	6.38	P63260	Actin, cytoplasmic 2
	3.92	P09041	Phosphoglycerate kinase 2
	5.36	P21300	Aldose reductase-related protein 1

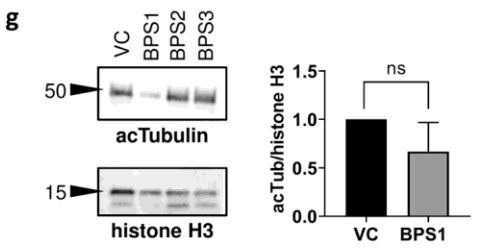

Fig. 4 Sperm acetylome and phosphorylome analyses. (a) Acetylated sperm proteins (acetylated lysine) with major bands. (b) Densitometric analysis of the ratio of candidate bands. (c) Phosphorylated sperm proteins (phosphorylated tyrosine) with major bands. (d) Densitometric analysis of the ratio of 100- to 85-kDa bands. (d') The ratio of 37–40-kDa (moderate) to 85–100-kDa (high) molecular weight bands. Differential counting was expressed as means (ranges) of three independent experiments. Differences were tested by two-way ANOVA, followed by Tukey's multiple comparison test, and asterisks indicate statistical significance *p<0.05, **p<0.01, ***p<0.001, and ****p<0.0001. (e) Candidate acetylated and (f) phosphorylated proteins from individual bands were evaluated using MALDI-TOF MS-based peptide detection. Analysed sperm samples represent a pool of three animals per experimental group from three independent replicates. (g) Densitometric analysis of acetylated tubulin from BPS1-treated sperm. VC: vehicle control, BPS1–3: increasing doses of bisphenol S

should be revised because alternative mechanisms of hormone-derived actions have been noted. For example, oestrogen-like action results in carcinogenesis [23], and changes in the distributions of oestrogen receptors and androgen-converting enzyme aromatase have been reported [24]. Endocrine disruptors have also been shown to modulate downstream signalling of activated G protein-coupled oestrogen receptors [25]. It is difficult to identify bisphenol-affected mechanisms after systemic exposure; therefore, cellular and molecular markers are appropriate for assessment of the risk of bisphenol exposure. Based on our findings, we speculate that different doses of BPS may have different effects. For example, whereas extremely low doses (BPS1: ~ 0.001 μg BPS/kg bw) affected sperm motility, higher BPS doses (BPS3: ~ 100 μg/kg bw) showed significant effects on testicular tissues. Surprisingly, moderate doses of BPS (BPS2: equal to daily intake of approx. 0.1 μg/kg bw) did not show any effects on spermiogram recording and histological assessment. This finding was consistent with the phenomenon of nonlinear effects [26], with the lowest dose of BPS (BPS1) inducing motility failure rather compared with the other BPS doses. Therefore, proteome profiling was used to test a wide range of BPS doses and characterise the dose-dependent mode of action.

Because of the lack of effect of BPS on the whole proteome of testicular tissues, protein acetylation and phosphorylation were chosen for further analysis. Although no significant effects were observed in terms of acetylation and phosphorylation of the detected peptides, γH2AX, a mark of DNA damage, was increased in BPS3 testicular tissues, demonstrating the increased occurrence of abnormalities. In sperm lysates, protein acetylation and phosphorylation were detected using specific antibodies against acetylated lysine and phosphorylated tyrosine. The choice of PTMs was consistent with the earlier described biological role of both PTMs in sperm capacitation and fertilisation ability [14, 27]. Indeed, altered levels of acetylated and phosphorylated proteins were observed after exposure to very-low-dose BPS (BPS1). This finding was presumably associated with decreased motility, resulting in detection of candidate proteins. We can assume that differentially acetylated and/or phosphorylated may be responsible for motility failure, in accordance with the significance of PTMs in major proteins, including phospho-hexokinase-1 [28] and phospho-outer dense fibre protein-2 [29]. Decreased phospho-tyrosine signals at 100 kDa suggest a lack of hexokinase-1 activity, which is associated with male infertility [30]. Our findings supported the mechanism of action of BPA described previously through fertility-related proteins, including protein phosphorylation [31]. Our study suggested that in addition to phosphorylation, bisphenols altered other PTMs, particularly protein acetylation. However, western blot analysis using anti-acetylated tubulin did not show any decrease, as expected, and other protein targets for acetylation were considered, including ATP synthase and actin, both of which are involved in sperm motility [32, 33].

Conclusion

In conclusion, these studies are among the first to raise the possibility that low and very low doses of BPS may have a deleterious effect on sperm quality in mammals. Since human BPS exposure is much lower (0.004 μg/kg bw/day) than is commonly tested [34], our findings suggest that post-translational effects could play a role in idiopathic infertility. Furthermore, this work supports the view that substitution of BPS for BPA may be inadequate for elimination of the negative effects of these agents on public health. Further biomonitoring and testing of molecular targets of BPS could be relevant for accurate risk assessment and elimination of its potential negative impact on male fertility.

Supplementary information

Supplementary information accompanies this paper at https://doi.org/10.1186/s12958-020-00596-x.

Additional file 1: Table S1. Composition of Whitten's HEPES-buffered medium. Table S2. Coefficients of error (CE) for evaluated terms of performed stereological analysis ($n = 9$ per each group). VC: vehicle control, BPS1-3: increasing doses of bisphenol S. Table S3. Hormone profiling of males in different experimental groups. Values of adrenocorticotropic hormone (ACTH), follicle-stimulating hormone (FSH), growth hormone (GH), luteinising hormone (LH), thyroid-stimulating hormone (TSH), cortisol, progesterone, testosterone, triiodothyronine (T3), and thyroxine (T4) are expressed as medians ± SEM, n = 5 per experimental group. Kruskal-Wallis tests were followed by Dunn's multiple comparison tests. Different letters in the same row indicate significant differences ($p < 0,05$). VC: vehicle control, BPS1-3: increasing doses of bisphenol S.

Abbreviations

BPA: Bisphenol A; BPS: Bisphenol S; CHAPS: 3-[(3-Cholamidopropyl) dimethylammonio]-1-propanesulfonate hydrate; MALDI-TOF MS: Matrix-assisted laser desorption ionisation time-of-flight mass spectrometry; MS: Mass spectrometry; nano-LC-MS: Nano-liquid chromatography mass spectrometry; PTMs: Post-translational modifications; TBS: Tris-buffered saline; VC: Vehicle control

Acknowledgements

We would like to thank Ms. Iveta Zimova for her kind help with the experimental work.

Ethics approval and consent to participate.

All animal procedures were done in accordance with the Protection of Animals against Cruelty (Act No. 246/1992) under the supervision of the Animal Welfare Advisory Committee at the Ministry of Education, Youth, and Sports of the Czech Republic.

Authors' contributions

Conceived project: JP, MK, JN. Animal experiment design: JN, OGA, PK. Execution of experiments: MŠ, NE, OGA, HŘ. Quantitative analyses of testes: YK, PRM, AMCT. Qualitative analyses of testes: MC. Proteome analysis: JM, JN, TF. Compiling the results: JN, MŠ, HŘ. Statistics: PH, JN, HŘ. Writing the manuscript and data interpretation: HŘ, MŠ, NJ, OGA. Proofreading: PRM. All authors read and approved the final manuscript.

Funding
This study was supported by the Czech Health Research Council (grant no. NV18–01-00544); the Charles University Research Fund (Progres Q39); the National Sustainability Programme I (NPU I) Nr. LO1503 provided by the Ministry of Education, Youth and Sports of the Czech Republic (MEYS CR); project no. SVV 02690 awarded by MEYS CR; and project no. CZ.02.1.01/0.0/0.0/16_019/0000787 "Fighting Infectious Diseases", awarded by MEYS CR and financed by The European Regional Development Fund, European Human Biomonitoring Initiative HBM4EU provided by H2020, and the United States Fulbright Commission (P001496 grant to P.R.M.).

Availability of data and materials
The datasets used and/or analyzed during the current study are available from the corresponding author on reasonable request.

Consent for publication
Not applicable.

Competing interests
The authors declare that they have no competing interests.

Author details
[1]Biomedical Center in Pilsen, Faculty of Medicine in Pilsen, Charles University, alej Svobody 1655/76, Pilsen, Czech Republic. [2]LR11ES41: Génétique, Biodiversité et Valorisation des Bioressources, Institut de Biotechnologie, Université de Monastir, 5000 Monastir, Tunisia. [3]Department of Histology and Embryology, Faculty of Medicine in Pilsen, Charles University, Pilsen, Czech Republic. [4]SaBio IREC (CSIC-UCLM- JCCM), Albacete, Spain. [5]SRC Biosciences & University of South Florida, Tampa, FL, USA. [6]Institute of Animal Science, 10-Uhrineves Prague, Czech Republic.

Received: 27 January 2020 Accepted: 22 April 2020
Published online: 28 May 2020

References
1. Siracusa JS, Yin L, Measel E, Liang S, Yu X. Effects of bisphenol a and its analogs on reproductive health: a mini review. Reprod Toxicol. 2018. https://doi.org/10.1016/j.reprotox.2018.06.005.
2. Rosenmai AK, Dybdahl M, Pedersen M, van Vugt-Lussenburg BMA, Wedebye EB, Taxvig C, et al. Are structural analogues to bisphenol a safe alternatives? Toxicol Sci. 2014. https://doi.org/10.1093/toxsci/kfu030.
3. Shi M, Sekulovski N, Ii JAM, Hayashi K. Effects of bisphenol a analogues on reproductive functions in mice. Reprod Toxicol. 2017. https://doi.org/10.1093/toxsci/kfz014.
4. Chen D, Kannan K, Tan H, Zheng Z, Feng Y-L, Wu Y, et al. Bisphenol analogues other than BPA: environmental occurrence, human exposure, and toxicity—a review. Environ Sci Technol. 2016. https://doi.org/10.1021/acs.est.5b05387.
5. Ullah H, Jahan S, Ain QU, Shaheen G, Ahsan N. Chemosphere effect of bisphenol S exposure on male reproductive system of rats: a histological and biochemical study. Chemosphere. 2016. https://doi.org/10.1016/j.chemosphere.2016.02.125.
6. Ullah A, Pirzada M, Jahan S, Ullah H, Shaheen G, Rehman H, et al. Bisphenol a and its analogs bisphenol B, bisphenol F, and bisphenol S: comparative in vitro and in vivo studies on the sperms and testicular tissues of rats. Chemosphere. 2018. https://doi.org/10.1016/j.chemosphere.2018.06.089.
7. Nevoral J, Kolinko Y, Moravec J, Žalmanová T, Hošková K, Prokešová Š, et al. Long-term exposure to very low doses of bisphenol S affects female reproduction. Reproduction. 2018. https://doi.org/10.1530/REP-18-0092.
8. Sidorkiewicz I, Czerniecki J, Jarząbek K, Zbucka-Krętowska M, Wołczyński S. Cellular, transcriptomic and methylome effects of individual and combined exposure to BPA, BPF, BPS on mouse spermatocyte GC-2 cell line. Toxicol Appl Pharmacol. 2018. https://doi.org/10.1016/j.taap.2018.09.006.
9. Ji K, Hong S, Kho Y, Choi K. Effects of bisphenol S exposure on endocrine functions and reproduction of zebrafish. Environ Sci Technol. 2013. https://doi.org/10.1021/es400329t.
10. Huang W, Zhao C, Zhong H, Zhang S, Xia Y, Cai Z. Bisphenol S induced epigenetic and transcriptional changes in human breast cancer cell line MCF-7. Environ Pollut. 2019. https://doi.org/10.1016/j.envpol.2018.12.084.
11. Pollard SH, Cox KJ, Blackburn BE, Wilkins DG, Carrell DT, Stanford JB, et al. Male exposure to bisphenol a (BPA) and semen quality in the home observation of Periconceptional exposures (HOPE) cohort. Reprod Toxicol. 2019. https://doi.org/10.1016/j.reprotox.2019.08.014.
12. Lawrence M, Daujat S, Schneider R. Lateral thinking: how histone modifications regulate gene expression. Trends Genet. 2016. https://doi.org/10.1016/j.tig.2015.10.007.
13. Brohi RD, Huo L-J. Posttranslational modifications in spermatozoa and effects on male fertility and sperm viability. Omi A J Integr Biol. 2017. https://doi.org/10.1089/omi.2016.0173.
14. Ritagliati C, Luque GM, Stival C, Baro Graf C, Buffone MG, Krapf D. Lysine acetylation modulates mouse sperm capacitation. Sci Rep. 2018. https://doi.org/10.1038/s41598-018-31557-5.
15. Naz RK, Rajesh PB. Role of tyrosine phosphorylation in sperm capacitation/acrosome reaction. Reprod Biol Endocrinol. 2004. https://doi.org/10.1186/1477-7827-2-75.
16. Rahman MS, Kwon WS, Karmakar PC, Yoon SJ, Ryu BY, Pang MG. Gestational exposure to bisphenol a affects the function and proteome profile of F1 spermatozoa in adult mice. Environ Health Perspect. 2017. https://doi.org/10.1289/EHP378.
17. Bachmanov AA, Reed DR, Beauchamp GK, Tordoff MG. Food intake, water intake, and drinking spout side preference of 28 mouse strains. Behav Genet. 2002. https://doi.org/10.1023/a:1020884312053.
18. Gundersen HJ, Jensen EB. The efficiency of systematic sampling in stereology and its prediction. J Microsc. 1987. https://doi.org/10.1046/j.1365-2818.1999.00457.x.
19. Mouton PR. Principles and practices of unbiased stereology: an introduction for bioscientists. Baltimore: Johns Hopkins University Press; 2002. p. 15–177.
20. Mouton PR. Unbiased stereology: a concise guide. Baltimore: Johns Hopkins University Press; 2011. p. 15–32.
21. Lanning LL, Creasy DM, Chapin RE, Barlow NJ, Regan KS, Mann PC, et al. Recommended approaches for the evaluation of testicular and Epididymal toxicity. Toxicol Pathol. 2002. https://doi.org/10.1080/01926230290105695.
22. Creasy DM. Evaluation of testicular toxicology: a synopsis and discussion of the recommendations proposed by the Society of Toxicologic Pathology. Birth Defects Res Part B Dev Reprod Toxicol. 2003. https://doi.org/10.1002/bdrb.10041.
23. Kim J, Choi H, Lee H, Lee G, Hwang K, Choi K. Effects of bisphenol compounds on the growth and epithelial mesenchymal transition of MCF-7 CV human breast cancer cells. J Biomed Res. 2017. https://doi.org/10.7555/JBR.31.20160162.
24. Žalmanová T, Hošková K, Nevoral J, Adámková K, Kott T, Šulc M, et al. Bisphenol S negatively affects the meotic maturation of pig oocytes. Sci Rep. 2017. https://doi.org/10.1038/s41598-017-00570-5.
25. Cao L-Y, Ren X-M, Li C-H, Zhang J, Qin W-P, Yang Y, et al. Bisphenol AF and Bisphenol B exert higher estrogenic effects than Bisphenol a via G protein-coupled estrogen receptor pathway. Environ Sci Technol. 2017. https://doi.org/10.1021/acs.est.7b03336.
26. Vandenberg LN, Colborn T, Hayes TB, Heindel JJ, Jacobs DR, Lee D-H, et al. Hormones and endocrine-disrupting chemicals: low-dose effects and nonmonotonic dose responses. Endocr Rev. 2012. https://doi.org/10.1210/er.2011-1050.
27. O'Flaherty C. Phosphorylation of the arginine-X-X-(serine/threonine) motif in human sperm proteins during capacitation: modulation and protein kinase a dependency. Mol Hum Reprod. 2004. https://doi.org/10.1093/molehr/gah046.
28. Nakamura N, Miranda-Vizuete A, Miki K, Mori C, Eddy EM. Cleavage of disulfide bonds in mouse Spermatogenic cell-specific type 1 hexokinase Isozyme is associated with increased hexokinase activity and initiation of sperm motility. Biol Reprod. 2008. https://doi.org/10.1095/biolreprod.108.067561.
29. Mariappa D, Aladakatti RH, Dasari SK, Sreekumar A, Wolkowicz M, van der Hoorn F, et al. Inhibition of tyrosine phosphorylation of sperm flagellar proteins, outer dense fiber protein-2 and tektin-2, is associated with impaired motility during capacitation of hamster spermatozoa. Mol Reprod Dev. 2009. https://doi.org/10.1002/mrd.21131.
30. Olds-Clarke P, Pilder SH, Visconti PE, Moss SB, Orth JM, Kopf GS. Sperm from mice carrying twot haplotypes do not possess a tyrosine phosphorylated form of hexokinase. Mol Reprod Dev. 1996;43:94–104.
31. Rahman MS, Kwon W-S, Lee J-S, Yoon S-J, Ryu B-Y, Pang M-G. Bisphenol-a affects male fertility via fertility-related proteins in spermatozoa. Sci Rep. 2015. https://doi.org/10.1038/srep09169.
32. Brener E, Rubinstein S, Cohen G, Shternall K, Rivlin J, Breitbart H. Remodeling of the actin cytoskeleton during mammalian sperm

capacitation and acrosome reaction. Biol Reprod. 2003. https://doi.org/10.1095/biolreprod.102.009233.
33. Ramió-Lluch L, Yeste M, Fernández-Novell JM, Estrada E, Rocha L, Cebrián-Pérez JA, et al. Oligomycin A-induced inhibition of mitochondrial ATP-synthase activity suppresses boar sperm motility and in vitro capacitation achievement without modifying overall sperm energy levels. Reprod Fertil Dev. 2014. https://doi.org/10.1071/RD13145.
34. Liao C, Liu F, Alomirah H, Loi VD, Mohd MA, Moon H-B, Nakata H, Kannan K. Bisphenol S in urine from the United States and seven Asian countries. Environ Sci Technol. 2012. https://doi.org/10.1021/es301334j.

Publisher's Note

A3

Řimnáčová H., Moravec J., Štiavnická M., Havránková J., Monsef L., Hošek P., Prokešová Š., Žalmanová T., Fenclová T., Petr J., Králíčková M., Nevoral J. 2022. Evidence of endogenously produced hydrogen sulfide (H_2S) and persulfidation in male reproduction. Submited to Scientific Reports.

Evidence of endogenously produced hydrogen sulfide (H_2S) and persulfidation in male reproduction

Hedvika Řimnáčová[1*], Jiří Moravec[1], Miriama Štiavnická[1,2], Jiřina Havránková[1,4], Ladan Monsef[1], Petr Hošek[1], Šárka Prokešová[3], Tereza Žalmanová[3], Tereza Fenclová[1], Jaroslav Petr[3], Milena Králíčková[1,4], Jan Nevoral[1,4]

[1]Biomedical Center in Pilsen, Faculty of Medicine in Pilsen, Charles University, Pilsen, Czech Republic
[2]Laboratory of Animal Reproduction, Department of Biological Sciences, Biomaterials Research Cluster, Bernal Institute, Faculty of Science and Engineering, University of Limerick, Limerick, Ireland
[3]Institute of Animal Science, Prague 10-Uhrineves, Czech Republic
[4]Department of Histology and Embryology, Faculty of Medicine in Pilsen, Charles University, Pilsen, Czech Republic.

***Correspondence.** Hedvika Řimnáčová. Biomedical Center in Pilsen, Faculty of Medicine in Pilsen, Charles University, Pilsen, Czech Republic, E-mail: Hedvika.rimnacova@lfp.cuni.cz

Abstract

Persulfidation contributes to a group of redox post-translational modifications (PTMs), which arise exclusively on the sulfhydryl group of cysteine as a result of hydrogen sulfide (H_2S) action. Redox-active molecules, including H_2S, contribute to sperm development; therefore, redox PTMs represent an extremely important signalling pathway in sperm life. In this path, persulfidation prevents protein damage caused by irreversible cysteine hyperoxidation and thus maintains this signalling pathway. In our study, we detected both H_2S and its production by all H_2S-releasing enzymes (cystathionine γ-lyase (CTH), cystathionine β-synthase (CBS), and 3-mercaptopyruvate sulfurtransferase (MPST)) in male reproduction, including spermatozoa. We provided evidence that sperm H_2S leads to persulfidation of proteins, such as glyceraldehyde-3-phosphate dehydrogenase, tubulin, and anchor protein A-kinase. Overall, this study suggests that persulfidation, as a part of the redox signalling pathway, is tightly regulated by enzymatic H_2S production and is required for sperm viability.

Introduction

Reactive oxygen species, reactive nitrogen species and reactive sulfur species (RONSS) are no longer considered harmful molecules leading to oxidative stress and apoptosis but are considered essential signalling molecules involved in many physiological events, such as sperm development, maturation, and capacitation[1–3]. Although a strong imbalance in redox reactions leads to damage and degradation of biomolecules, one molecule handles these conditions surprisingly well. Indeed, cysteine, a common amino acid incorporated into proteins, is the main player in the establishment of protein structure and antioxidant defence due to its sulfhydryl group (-SH) and its alternative modifications. In particular, the scavenging of RONSS through redox post-translational modifications (PTMs) of cysteine benefits the protein lifespan. Cysteine residues can be easily oxidized, and their oxidation is mostly reversible, which makes redox PTMs of cysteine unique signalling molecules. Moreover, these modifications often depend on each other, and one PTM leads to another, suggesting cross-regulation between individual redox PTMs[4,5]. For example, antioxidant enzymes are usually regulated by redox PTMs of cysteine under stress conditions. While S-nitrosylation (-SNO) and S-sulfenylation (-SOH) of -SH activate enzymes, irreversible hyperoxidation to sulfinic ($-SO_2H$) and sulfonic ($-SO_3H$) acids

deactivates them. Additionally, proteins are rescued from irreversible hyperoxidation due to the reduction of SNO/SOH by glutathione (GSH) to form S-glutathionylation (-SSG)[6,7]. Persulfidation (-$(S)_nH$) has the same rescue effect and thus plays an indisputable role in protein signalling across many tissues[8,9]. Accordingly, several proteins important for sperm physiology have been reported as -SNO targets[2,10]. Since -SNO could serve as a -$(S)_nH$ precursor, we can assume that -$(S)_nH$ will affect the activity of the proteins. Interestingly, no one has detected persulfidated proteins in spermatozoa, and the role of -$(S)_nH$ in male reproduction remains elusive. Although certain PTMs promote persulfidation of cysteine, this modification requires the action of hydrogen sulfide (H_2S). H_2S is physiologically produced in various cells by three specific enzymes from cysteine and homocysteine: cystathionine γ-lyase (CTH), cystathionine β-synthase (CBS), and 3-mercaptopyruvate sulfurtransferase (MPST). Notably, cysteine is the main target of H_2S action and an important source of H_2S. All these facts indicate that cysteine has a very unique role in H_2S metabolism. Although H_2S-releasing enzymes were detected in mouse testes[11] and CBS and CTH in human spermatozoa[12], complete knowledge about their distribution through mammalian spermatozoa is lacking.

Taken together, the results of previous studies indicate that endogenous production of H_2S is associated with antioxidant defence and antiapoptotic and antiaging events reported in many tissues[13]. Unfortunately, studies on testicular tissue and spermatozoa are limited by the artificial supply of H_2S rather than real H_2S production[11,12,14,15]. Therefore, recent findings are unclear, and there are different conclusions depending on the donor concentration used. Although endogenous H_2S production has been overlooked in male reproduction, these studies suggest that it has potential in reproductive physiology and deserves further attention. Our study provides the first evidence of physiological H_2S production in spermatozoa and physiological contributions in the form of persulfidation in sperm physiology.

Results

Redox PTMs of cysteine do not drive maturation of male reproduction. In this experiment, we focused on persulfidation in the broad context of other redox PTMs (-SNO and -SOH), in which cross regulations with persulfidation have been reported[4,5]. Due to the physiological contribution of cysteine PTMs in sperm maturation, we assumed that redox PTMs control the onset of spermatogenesis and thus drive sexual maturity in males. Therefore, we compared testicular lysates from mouse males before puberty onset, 21-day-old (young) and fully matured, 12-14-week-old males (adult) by Western blot (WB) detection of cysteine modifications: -SNO, -SOH, and -$(S)_nH$ (Fig. 1). We did not find any differences between the young and adult groups in i) protein distribution (Fig. 1a – d), ii) individual band intensity (Fig. 1e – g) or iii) the total protein intensity (Fig. 1h – j) in any of the following parameters, suggesting that redox PTMs do not drive male reproductive maturation. The WBs of each PTM showed a specific ladder of bands (Fig. 1a – d). There was no band detected concurrently for -SNO/-SOH and -$(S)_nH$, which suggests that there are different abundant proteins undergoing the specific PTMs, e.g., -SNO, -SOH, or -$(S)_nH$. For instance, 55- and 75-kDa bands (Fig. 1d) were not detected, nor was -SNO or -SOH as intense as -$(S)_nH$. This observation indicates that H_2S is able to react and modify most -SNOs and -SOHs of certain proteins to form -$(S)_nH$. -$(S)_nH$ was found in a small number of proteins compared with the detected sulfhydryl groups (-SH) (Fig. 1c, 1j). Thus, -$(S)_nH$ apparently does not drive male maturation, and it modifies exclusive proteins regardless of the maturity of testicular tissue.

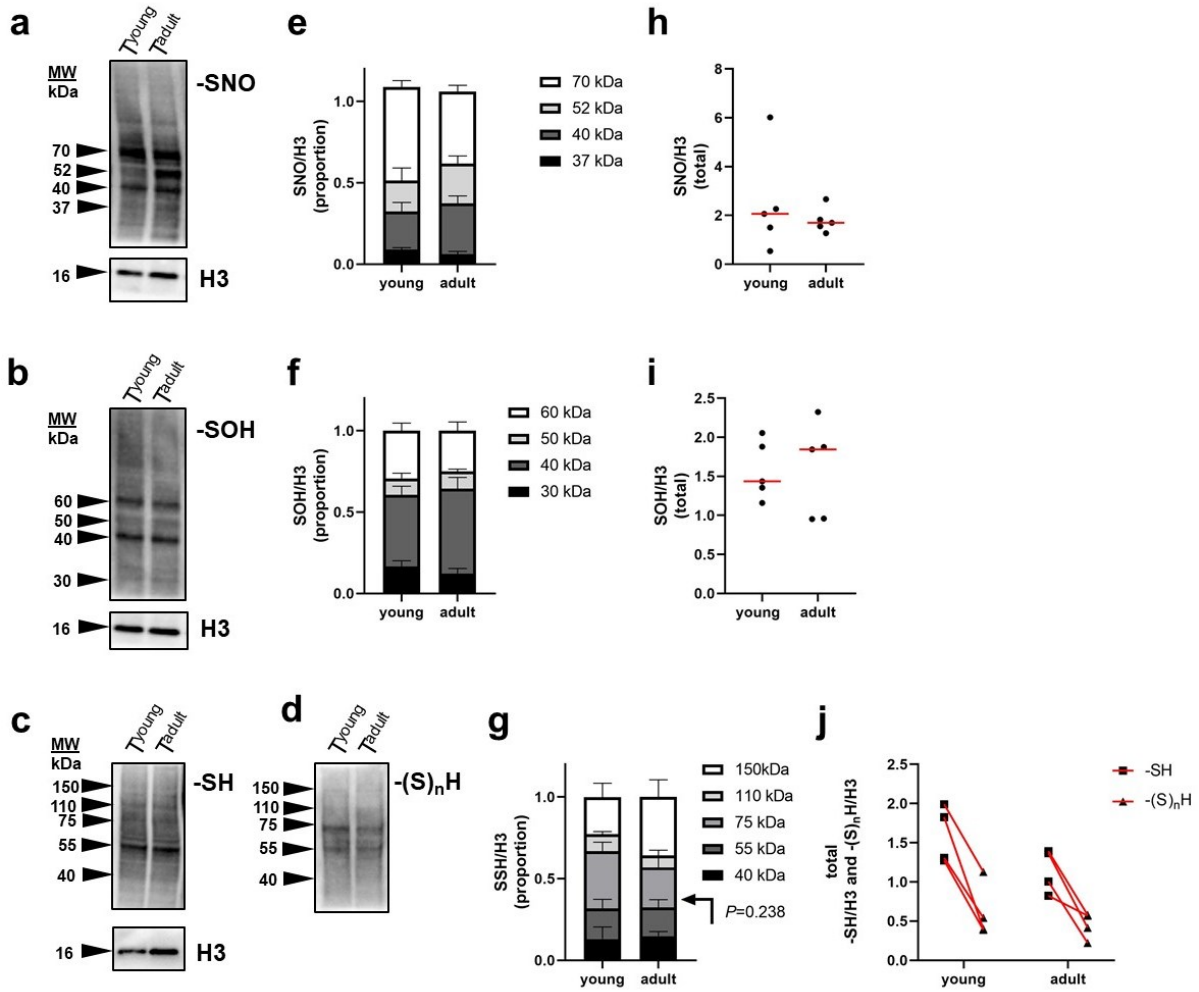

Figure 1. Detection of S-nitrosylation (-SNO), S-sulfenylation (-SOH), free thiols (-SH), and persulfidation (-$(S)_nH$), redox PTMs of proteins, in young (i.e., prepubertal) and adult mouse testes. **(a – d)** Western blot detection of SNO, -SOH, -SH and -$(S)_nH$. **(e – g)** Densitometric analysis of abundant bands **(h – j)** Total density of abundant bands is expressed and young and adult males were compared; each dot represents an individual. **(j)** -SH and -$(S)_nH$ belonging to the same individual are connected by a red line. Histone 3 (H3) was used as a housekeeping internal control.

Persulfidation is abundant in testes compared to other tissues. Persulfidation (-$(S)_nH$) plays a plausible role in ageing, apoptosis and stress defence in many tissues, but information about this PTM in male reproduction is still missing. To shed light on this issue, we performed quantitative and qualitative analyses of -$(S)_nH$ in the testis. Because no specific maturity-dependent protein pattern was observed, the index of -$(S)_nH$ was compared in different kinds of tissues. We selectively labelled -$(S)_nH$, accordingly with[16] with slight modifications, while free -SH groups were blocked by MMTS and subsequently the -$(S)_nH$ groups were alkylated by IAM-PEG-biotin (Fig. 2a). Biotin was detected by streptavidin conjugated with horseradish peroxidase *via* WB detection (Fig. 2b). We observed that -$(S)_nH$ ranged from 40 to 150 kDa in the testes of adult mice. To validate the specificity of the method used, we prepared three specifically treated groups to detect: $(S)_nH$+SH (no MMTS treatment), -$(S)_nH$ only (MMTS-treated), and naturally biotinylated proteins (nonalkylated control). The detected persulfidated proteins were then identified using pulldown assays and nano-LC-MS (Fig. 2c, 2d). We compared persulfidated proteins from the testis with those of the brain and liver, in which -$(S)_nH$ was

previously widely described (Fig. 2c). We found proteins that were conservatively persulfidated across the tissues, but we found 68 proteins that were persulfidated only in the testis. Fig. 2d represents persulfidated proteins specifically found in testes in the size range 55–75 kDa (bands in white rectangle marked with * in Fig. 2b). These findings suggest that -$(S)_n$H targets proteins specifically in the testis, although these are widely expressed proteins.

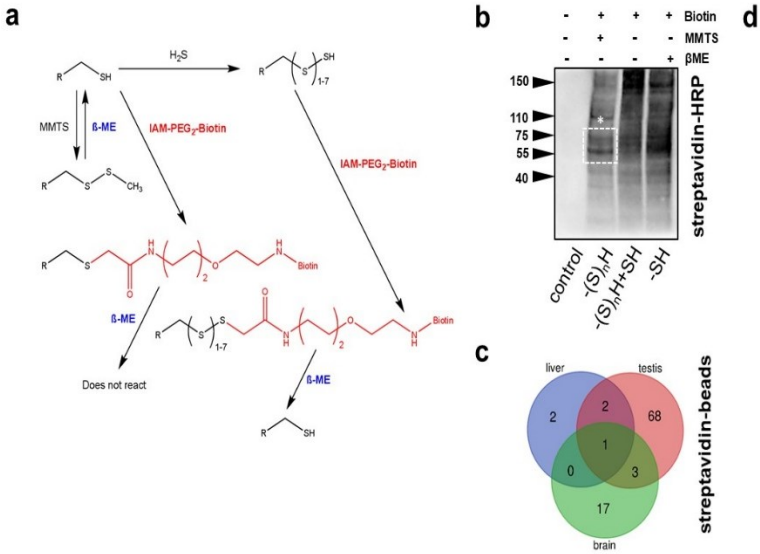

d

Entry	Entry name	Protein name	Length (AA)	Mass (kDa)
P09103	PDIA1_MOUSE	Protein disulfide-isomerase	509	57,058
P17156	HSP72_MOUSE	Heat shock-related 70 kDa protein 2	633	69,642
P20029	BIP_MOUSE	Endoplasmic reticulum chaperone BiP	655	72,422
P35564	CALX_MOUSE	Calnexin	591	67,278
P10126	EF1A1_MOUSE	Elongation factor 1-alpha 1	462	50,114
P24549	AL1A1_MOUSE	Retinal dehydrogenase 1	501	54,468
Q03265	ATPA_MOUSE	ATP synthase subunit alpha, mitochondrial	553	59,753
P52480	KPYM_MOUSE	Pyruvate kinase PKM	531	57,845
P63038	CH60_MOUSE	60 kDa heat shock protein, mitochondrial	573	60,955
P27773	PDIA3_MOUSE	Protein disulfide-isomerase A3	505	56,678
Q8BMF4	ODP2_MOUSE	Dihydrolipoyllysine-residue acetyltransferase	642	67,942
Q9Z2I9	SUCB1_MOUSE	Succinate-CoA ligase subunit beta, mitochondrial	463	50,114
P20152	VIME_MOUSE	Vimentin	466	53,688
P42932	TCPQ_MOUSE	T-complex protein 1 subunit theta	548	59,555
P80315	TCPD_MOUSE	T-complex protein 1 subunit delta	539	58,066
Q9DA79	DPEP3_MOUSE	Dipeptidase 3	493	54,247
Q06890	CLUS_MOUSE	Clusterin (Apolipoprotein J)	448	51,656
P80314	TCPB_MOUSE	T-complex protein 1 subunit beta	535	57,477
P61979	HNRPK_MOUSE	Heterogeneous nuclear ribonucleoprotein K	463	50,976
P47738	ALDH2_MOUSE	Aldehyde dehydrogenase, mitochondrial	519	56,538
P11983	TCPA_MOUSE	T-complex protein 1 subunit alpha	556	60,449
Q9JHU9	INO1_MOUSE	Inositol-3-phosphate synthase 1	557	60,932
P80316	TCPE_MOUSE	T-complex protein 1 subunit epsilon	541	59,624
P32037	GTR3_MOUSE	Solute carrier family 2, transporter member 3	493	53,479
P80318	TCPG_MOUSE	T-complex protein 1 subunit gamma	545	60,630
P06801	MAOX_MOUSE	NADP-dependent malic enzyme	572	63,954

Figure 2. Persulfidation in mouse tissues with emphasis on testis. (**a**) Principle of selective detection of persulfidation (-$(S)_n$H) using the thiol-selective binding ability of S-methyl methanethiosulfonate (MMTS) and the binding affinity of IAM-PEG-biotin to thiols (-SH). (**b**) β-Mercaptoethanol (β-ME), a reducing agent, was used to eliminate persulfide-biotin bonds and selectively detect free thiols. Bands in the size range 55–75 kDa (*) belonging to abundant proteins modified by -$(S)_n$H. **(c)** Alternatively, selectively labelled -$(S)_n$H with IAM-PEG-biotin was loaded on streptavidin-coated agarose beads. The eluted native proteins were digested and detected by nano-LC-MS. Liver, brain, and testicular tissues were processed *via* pulldown assays and nano-LC-MS detection, and persulfidated proteins were compared and expressed *via* Venn diagram. (**d**) Proteins of 55-75 kDa are presented in the table.

H2S-releasing enzymes are present in germ cells independent of their maturation stages in mouse testes. We found that persulfidation (-$(S)_n$H) is relatively abundant in the testes compared to the frequently studied liver and brain. -$(S)_n$H is a well-known result of H_2S action, and it is released enzymatically inside the cell. Therefore, we consider monitoring H_2S production to be essential (Fig. 3). CBS, CTH and MPST have been previously detected in mouse testes[11], but their distribution across developmental stages of germ cells has not been determined. Therefore, immunofluorescence detection of CBS, CTH, and MPST in testis sections was performed, depending on the developmental stages of germ cells within the seminiferous epithelial cycle. The results showed a strong dependency of enzymes on the cytoplasm of developing germ cells, regardless of the cell type and phase of spermiogenesis, distinguished in the Golgi, cap, and acrosomal stage (Fig. 3a). Enzyme independence of germ cell maturation was confirmed by WB performed on prepubertal and adult mice (Fig. 3b, c). The observation that H_2S is not apparently associated with maturity level supports the versatility of H_2S action in a cell. To elucidate H_2S enzymatic production in testicular tissue, we performed colorimetric H_2S detection (Fig. 3d). After the addition of pyridoxal-5'-phosphate (PxP), a cofactor of CBS and CTH, and L-cysteine, the substrate of enzymes, into the testis lysate, the production of H_2S increased. To the best of our knowledge, we are the first to describe the relationship among H_2S

appearance, the enzymes responsible for its production, and the -$(S)_nH$ of proteins of male reproduction. Moreover, the association of H_2S-releasing enzymes in germ cells predicts H_2S production in fully differentiated spermatozoa and the possible role of -$(S)_nH$ in sperm physiology.

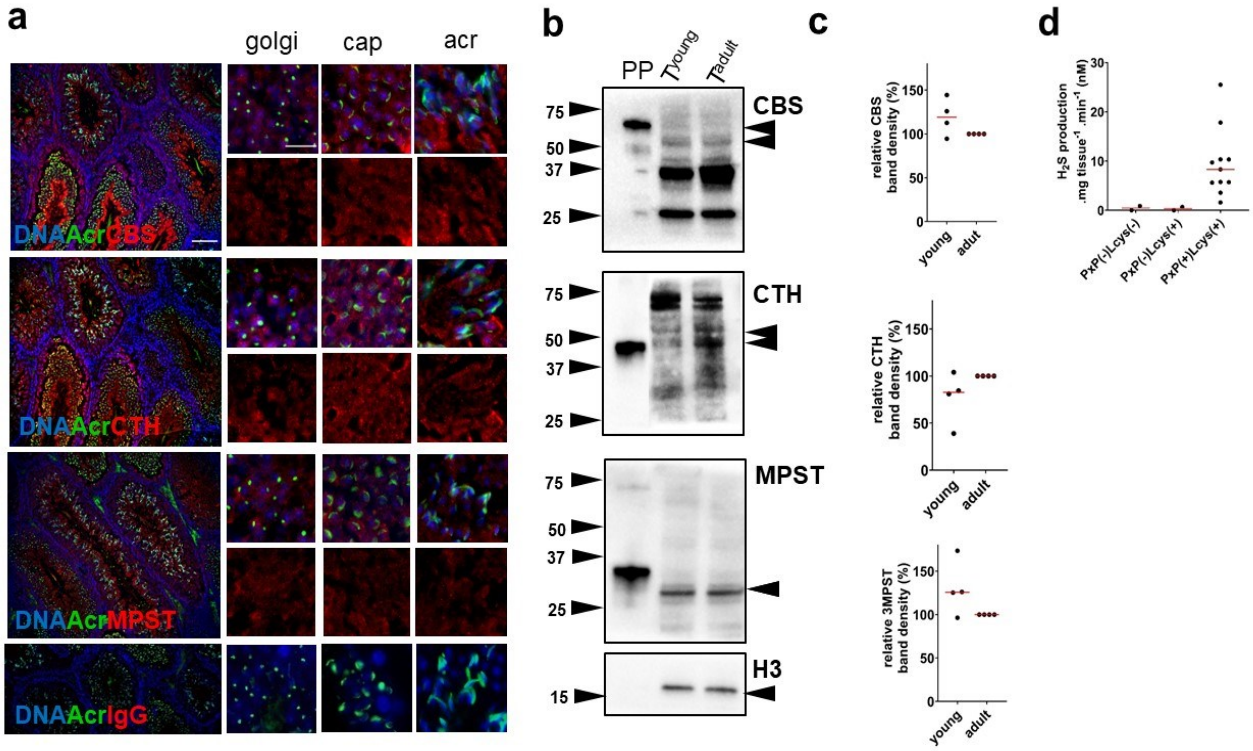

Figure 3. Detection of H_2S-releasing enzymes in mouse testis: **(a)** Immunofluorescence of testis sections. Acrosomal development stages of spermatids were recognized using PNA (200x). Individual stages of acrosomal biogenesis, representing the Golgi, cap, and acrosomal (Acr) stages, are emphasized (1000x). Scale bar 100 µm. (**b**) Cystathionine β-synthase (CBS), cystathionine γ-lyase (CTH) and 3-mercaptopyruvate sulfurtransferase (MPST) were detected by Western blot**. (c)** The comparison of prepubertal (young) and adult males was performed. **(d)** Colorimetric detection of H_2S production in testes, which increased after the addition of pyridoxal-5'-phosphate (PxP) and L-cysteine.

Enzymatic production of H_2S leads to persulfidation of protein cysteine in mouse spermatozoa. The aim of this experiment was to examine H_2S-releasing enzymes in mouse spermatozoa during their passage through the caput into the cauda epididymis. For analysis of H_2S production, we compared the pattern of H_2S-releasing enzyme subcellular distribution with H_2S fluorescence visualization and protein persulfidation (-$(S)_nH$) in fully differentiated spermatozoa. First, we detected CBS, CTH, and MPST *via* WBs in mouse spermatozoa from the caput epididymis (Sp^{caput}) and cauda epididymis (Sp^{cauda}) (Fig. 4a). Caput spermatozoa showed a strong signal of all H_2S-releasing enzymes, whereas caudal spermatozoa showed either decreased (CBS), weak (MPST) or almost no signal (CTH) detected by WBs. To enhance the observation of H_2S-releasing enzymes in caudal spermatozoa, we performed immunocytochemistry of single sperm cells (Fig. 4b – d). The signal of all enzymes along the entire length of the flagella was observed in caudal spermatozoa. Their enzymatic action was proved by H_2S labelling by specific Sulfane Sulfur Probe 4 (SSP4) (Fig. 4e). Similar to H_2S-releasing enzymes, the signal was emitted in the entire length of the flagella with the highest intensity in the midpiece. The observation of H_2S production corresponding to H_2S-releasing enzyme locations strongly supports the occurrence of H_2S enzymatic production. Finally, we detected -$(S)_nH$ and found it exclusively in the

midpiece (Fig. 4f). Although -$(S)_nH$ showed a slightly different pattern than H_2S-releasing enzymes, it perfectly followed the site of the highest occurrence of H_2S production. Therefore, we identified the midpiece as the location of H_2S enzymatic activity, H_2S production, and biochemical action.

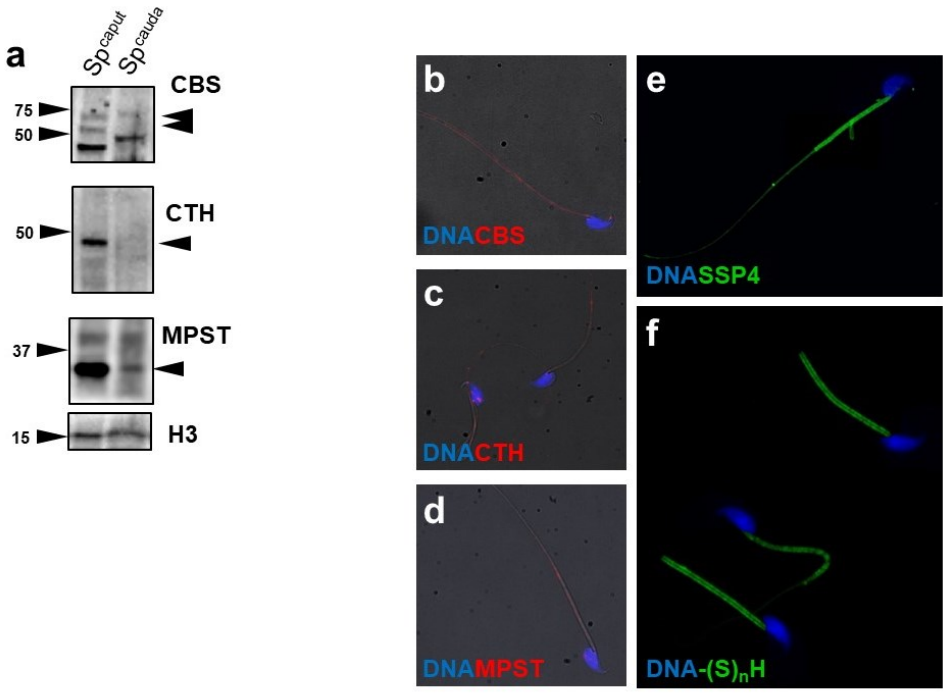

Figure 4. Production of H_2S, its enzymes and persulfidation (-$(S)_nH$) in mouse spermatozoa. **(a)** Western blot detection of cystathionine β-synthase (CBS), cystathionine γ-lyase (CTH) and 3-mercaptopyruvate sulfurtransferase (MPST) in mouse spermatozoa during their maturation in the epididymis. **(b – d)** Immunocytochemistry of CBS, CTH and MPST. **(e)** Localization of H_2S production by Sulfane Sulfur Probe 4 (SSP4) and **(f)** -$(S)_nH$. Spermatozoa were magnified (1000x).

Sperm H_2S-releasing enzymes produce H_2S in spermatozoa across mammalian species. Based on previous findings of H_2S production and the expression of H_2S-releasing enzymes in mouse testes and spermatozoa, we suggest that H_2S is enzymatically produced in spermatozoa across mammalian species. Therefore, we detected CBS, CTH, and MPST in human spermatozoa and in mouse and pig spermatozoa, the most common mammalian models. Enzyme detection was followed by elucidation of the release of SSP4-labelled H_2S. Based on the known species-specific molecular weight of the individual enzymes based on the UniProtKB Database (Fig. 5a, see the phylogenetic trees in Supplementary Fig. S1), we identified all enzymes *via* WBs (Fig. 5b, see Supplementary Fig. S2 for whole WB membrane). Although immunocytochemistry of H_2S-releasing enzymes showed interspecies variability in subcellular distribution, H_2S production (SSP4) is quite constant in humans (Fig. 5c) and boars (Fig. 5d). This finding suggests that there is a different composition of the H_2S-releasing enzymes responsible for most H_2S production in a species-dependent manner. While H_2S production colocalized with CTH in human spermatozoa, in boar spermatozoa, it colocalized instead with MPST. Sequential disappearance of H_2S-releasing enzymes through spermatozoa maturation was shown by the evoked capacitation (Fig. 5e) and zona pellucida-binding assays of boar spermatozoa undergoing the acrosomal reaction, the last step of sperm maturation (Fig. 5f). This result complements our previous finding that H_2S-releasing enzymes gradually decrease from spermatozoa during their maturation in the epididymis (Fig. 4a). Based on these observations, we conclude that the presence of

191 H_2S-releasing enzymes is partially lost from the cytoplasmic membrane during remodelling, which
192 accompanies sperm maturation. Therefore, these enzymes do not appear to be involved in the sperm
193 fertilization of eggs.

a

Species	CBS (isoform 1/2)	CTH (isoform 1/2)	MPST (isoform 1/2)
Mus musculus	61,540/60,190 Da	43,560 Da	33,100 Da
Sus scrofa	66,980 Da	44,490 Da	34,200 Da
Homo sapiens	60,590/61860 Da	44,500/39,510 Da	33,160/35,250 Da

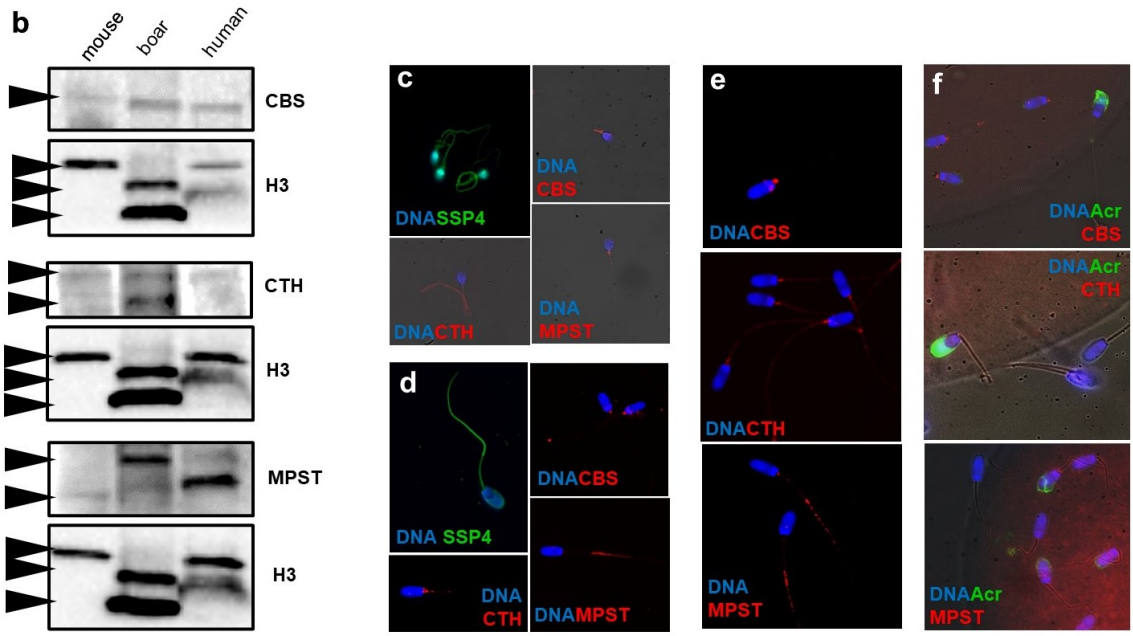

194

195 **Figure 5.** Interspecies production of H_2S-releasing enzymes and H_2S. **(a)** Species-specific molecular
196 weight of the individual enzymes. **(b)** Western blot detection of CBS, CTH and MPST in human, boar
197 and mouse spermatozoa. **(c)** Immunocytochemistry of all H_2S-releasing enzymes and detection of H_2S
198 production by the SSP4 probe in human and **(d)** boar spermatozoa. **(e)** Decreases in CBS, CTH and
199 MPST signal intensity during the last steps of boar sperm maturation, capacitation and **(f)** acrosomal
200 reaction during sperm-*zona pellucida* binding. Spermatozoa were emphasized (1000x)

201 **Distribution and identification of persulfidates in human spermatozoa.** In accordance with the
202 aforementioned presence of H_2S-releasing enzymes and H_2S, we investigated the effects of H_2S on
203 persulfidation (-$(S)_nH$) in the sperm protein of three normozoospermic donors using the approach
204 described above. Concurrently, all three samples were subjected to flow cytometry analysis to obtain
205 an overview of persulfidation occurrence across the entire sperm population. We observed -SH and -
206 $(S)_nH$ with regard to plasma membrane integrity (PMI) using flow cytometry (Fig. 6a). In the control
207 groups, spermatozoa were separated into three subpopulations according to susceptibility to PMI and
208 6-IAF staining as follows: the 1st quadrant (Q1) was live spermatozoa highly positive for 6-IAF, the
209 2nd quadrant (Q2) was dead spermatozoa highly positive for 6-IAF and the 4th quadrant (Q4) was live
210 spermatozoa slightly positive for 6-IAF. When free thiols (*i.e.,* -SH) were specifically blocked in the
211 MMTS experimental group, most 6-IAF signals disappeared, and spermatozoa moved to the less
212 intense 6-IAF quadrants Q3 (death) and Q4 (live). This observation was supported by the detection of
213 -SH and -$(S)_nH$ *in situ*, occurring in whole sperm or exclusively in the midpiece in the control (Fig.

214 6b). Following free thiol blocking, the sperm head-rich signal disappeared. For both flow cytometry
215 and *in situ* detection, cell death was noticeably accompanied by substantial thiol exposure through the
216 spermatozoon, while persulfidation was stably localized in the midpiece independent of live or dead
217 sperm status. This observation was supported by the analysis of three independent semen donors, while
218 the analysis was performed on the subpopulation of live spermatozoa (*i.e.,* Q1 and Q4 quartiles). There
219 was a small population of spermatozoa (4.6–5.1%) showing high signal intensity belonging to -SH and
220 $-(S)_nH$ in the control group. When -SH was blocked, only $-(S)_nH$ remained, and significantly weaker
221 signals were detected in the sperm population in the MMTS group (Fig. 6c). Using the biotin-switched
222 detection of $-(S)_nH$ in sperm lysate, we found that the abundance of persulfidated proteins did not show
223 any capacitation-dependent difference (Fig. 6d), similar to our findings achieved in other mammalian
224 models (Supplementary Fig. S3). Concurrently, these persulfide-labelled samples were subjected to
225 pulldown assays, followed by nano-LC-MS peptide detection. We identified 37 persulfidated proteins
226 with 99% confidence, in most cases being in a donor-specific pattern (Fig. 6f). Five proteins were
227 found to match at least in two donors, marked in bold in the table containing all characterized
228 persulfidated sperm proteins (Fig. 6e). Altogether, nano-LC-MS findings of midpiece-occurring
229 proteins are in accordance with the H_2S-releasing enzyme distribution, H_2S labelling and *in situ*
230 detection of persulfidation, underlining the spatiotemporal requirement of H_2S activity in target protein
231 modulation.

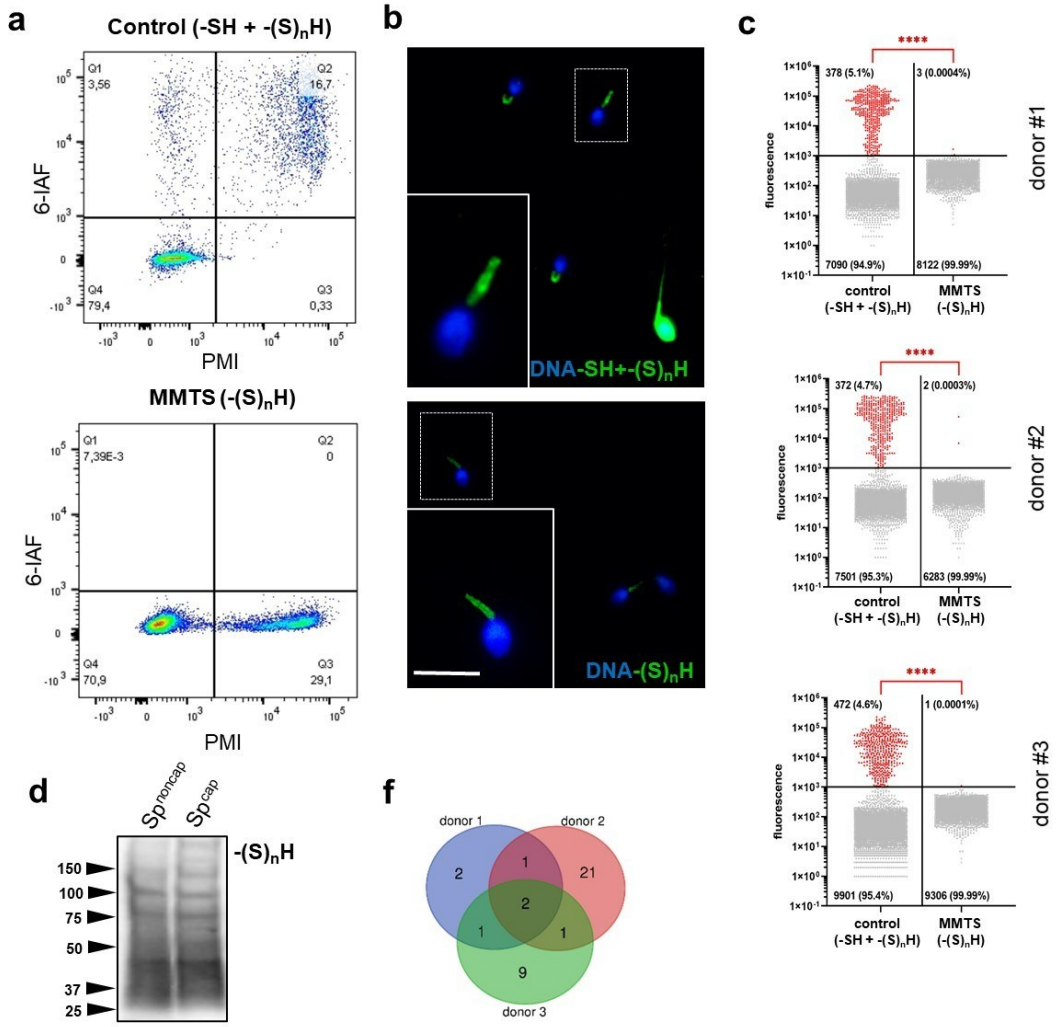

e

Entry	Entry name	Proteins names	Length (AAA)	Mass (Da)
Q5JQC9	**AKAP4_HUMAN**	**A-kinase anchor protein**	**854**	**94,477**
O14556	**G3PT_HUMAN**	**Glyceraldehyde-3-phosphate dehydrogenase testis-specific**	**408**	**44,501**
P07864	**LDHC_HUMAN**	**L-lactate dehydrogenase C chain**	**332**	**36,311**
Q02383	**SEMG2_HUMAN**	**Semenogelin-2**	**582**	**65,444**
Q6PEY2	**TBA3E_HUMAN**	**Tubulin alpha-3E chain**	**450**	**49,859**
P07288	KLK3_HUMAN	Prostate-specific antigen	261	28,741
Q9BQE3	TBA1C_HUMAN	Tubulin alpha-1C chain	449	49,895
Q13275	SEM3F_HUMAN	Semaphorin-3F	785	88,381
Q9BUN1	MENT_HUMAN	Protein MENT	341	36,769
P21266	GSTM3_HUMAN	Glutathione S-transferase Mu 3	225	26,560
P41229	KDM5C_HUMAN	Lysine-specific demethylase 5C	1560	175,720
P14618	KPYM_HUMAN	Pyruvate kinase PKM	531	57,937
Q5JX71	F209A_HUMAN	Protein FAM209A	171	19,603
P10323	ACRO_HUMAN	Acrosin	421	45,847
P06733	ENOA_HUMAN	Alpha-enolase	434	47,169
P01266	THYG_HUMAN	Thyroglobulin	2768	304,790
P37802	TAGL2_HUMAN	Transgelin-2	199	22,391
P98164	LRP2_HUMAN	Low-density lipoprotein receptor-related protein 2	4655	521,958
P04075	ALDOA_HUMAN	Fructose-bisphosphate aldolase A	364	39,420
Q9NY87	SPNXC_HUMAN	Sperm protein associated with the nucleus on the X chromosome C	97	10,982
Q9HCE0	EPG5_HUMAN	Ectopic P granules protein 5 homolog	2579	292,481
Q9Y5B0	CTDP1_HUMAN	RNA polymerase II subunit A C-terminal domain phosphatase	961	104,399
P49916	DNLI3_HUMAN	DNA ligase 3 OS=Homo sapiens	1009	112,907
Q9BS86	ZPBP1_HUMAN	Zona pellucida-binding protein 1	351	40,142
Q8IXK0	PHC2_HUMAN	Polyhomeotic-like protein 2	858	90,713
Q67FW5	B3GNL_HUMAN	UDP-GlcNAc:betaGal beta-1 3-N-acetylglucosaminyltransferase-like protein 1	361	40,713
Q9UPI3	FLVC2_HUMAN	Feline leukemia virus subgroup C receptor-related protein 2	526	57,241
Q9H0C2	ADT4_HUMAN	ADP/ATP translocase 4	315	35,022
P10909	CLUS_HUMAN	Clusterin	449	52,495
P46439	GSTM5_HUMAN	Glutathione S-transferase Mu 5	218	25,675
Q9BXN6	SPNXD_HUMAN	Sperm protein associated with the nucleus on the X chromosome D	97	11,029
P02768	ALBU_HUMAN	Albumin OS=Homo sapiens	609	69,367
Q5VTE0	EF1A3_HUMAN	Putative elongation factor 1-alpha-like 3	462	50,185
Q6UW49	SPESP_HUMAN	Sperm equatorial segment protein 1	350	38,931
Q9Y696	CLIC4_HUMAN	Chloride intracellular channel protein 4	253	28,772
P04279	SEMG1_HUMAN	Semenogelin-1	462	52,131
P54652	HSP72_HUMAN	Heat shock-related 70 kDa protein 2	639	70,021

232

Figure 6. Free thiols and persulfidation analysis of proteins in human spermatozoa. **(a)** Flow cytometry of thiols (-SH) and persulfidation (-$(S)_nH$) in spermatozoa due to 6-iodoacetamidofluorescein (6-IAF) staining without (control) and with (MMTS) blocking of free thiols. The dot plot shows the separation of sperm subpopulations according to plasma membrane integrity (PMI) and 6-IAF signal intensity. (**b**) Representative images of -SH and -$(S)_nH$ detection *in situ* showing 6-IAF staining patterns in the MMTS and control groups. The white rectangle indicates the -$(S)_nH$-assumed signal in the midpiece of emphasized spermatozoa (scale bar: 10 μm). Spermatozoa were emphasized (1000x). **(c)** Presence of -SH+-$(S)_nH$ in the control and -$(S)_nH$ in the MMTS groups in live spermatozoa of three donors. Differences between the fluorescent signals belonging to -SH+-$(S)_nH$ and -$(S)_nH$. Dots represent the fluorescence signal of individual spermatozoa. Lines express the mean of measured spermatozoa tested on live sperm subpopulations using the one-sample Wilcoxon test (****, $P < 0.0001$). **(d)** Persulfidated proteins separated by molecular weight in human spermatozoa being noncapacitated ($Sp^{non\text{-}cap.}$) or capacitated (Sp^{cap}). **(e)** All detected persulfidated proteins are shown in the table. Persulfidated proteins that matched at least in two donors are shown in bold. (**f**) Venn diagram shows 37 persulfidated proteins identified in three independent donors by nano-LC-MS.

Discussion

The sulfhydryl group (-SH) of cysteine provides a unique signalling pathway in which many redox molecules are involved. These molecules, such as nitric oxide (NO), hydrogen peroxide (H_2O_2) or hydrogen sulfide (H_2S), oxidize or reduce -SH to form various redox post-translational modifications (PTMs) that control protein activity. These redox PTMs are unstable and continuously replacing each other on cysteine and together creating sophisticated signalling pathways. Persulfidation (-$(S)_nH$) plays a central role in this pathway, as it replaces S-nitrosylation (-SNO) and S-sulfenylation (-SOH) on cysteine and thus regulates not only protein activities but also prevents their inactivation by hyperoxidation. There are many proteins that are regulated by redox PTMs in male reproduction[2,10] but -$(S)_nH$ has not been investigated. In this study, we identified the existence of -$(S)_nH$ and its relation to endogenous H_2S production and H_2S-releasing enzyme localization in male reproduction with a focus on spermatozoa.

To the best of our knowledge, our study is the first to identify the protein -$(S)_nH$ in mouse testes and human spermatozoa. Subsequently, we compared persulfidated (-$(S)_nH$) proteins found in mouse testes with -$(S)_nH$ from previously widely studied tissues, the brain and liver (Fig. 2c). Surprisingly, the largest amount of -$(S)_nH$ was detected in the testis, and 68 of the proteins were persulfidated uniquely in the testis (Fig. 2d). Although these proteins are not exclusive to the testes, they are apparently persulfidated in the testis only. It is well known that -$(S)_nH$ is the result of H_2S action, and partially due to this effect, artificial supplementation of H_2S has antiaging and antioxidant effects in many tissues, including spermatozoa[11,12,14]. There are several publications addressing H_2S donor efficacy, although supplementation with exogenous H_2S has possible toxic effects[15]. In contrast to these publications, there is no evidence about physiological endogenous H_2S production and its consequences for male reproduction. Although all H_2S-releasing enzymes have been previously detected in mouse testis[11] and CBS and CTH in human spermatozoa[12] and rat epididymis[17], we immunodetected all three responsible enzymes in mouse testicular cross-sections and in spermatozoa of three mammalian species. Therefore, we claimed that enzymes are distributed in the cytoplasm regardless of the cell type or germ cell maturation stage. Although there was a steady distribution of enzymes across the seminiferous epithelium cycle, our experiments showed that spermatozoa from caput showed a higher intensity of H_2S-releasing enzymes than more mature caudal spermatozoa (Fig. 4a). Spermatozoa obviously lose their H_2S-releasing enzymes during passage through the epididymis. An interesting finding was made by a study describing the importance of H_2S production for sperm quiescence in the rat epididymis[17]. In contrast to that in spermatozoa, the expression of CBS and CTH

281 was increased towards the cauda epididymis[17]. Based on recent knowledge, the epididymal epithelium
282 appears to compensate for sperm H_2S-releasing enzyme loss during spermatozoa passage through the
283 epididymis by increasing the self-production of enzymes. Nevertheless, the loss of H_2S-releasing
284 enzymes continues beyond the epididymis and is found in further steps of sperm maturation,
285 capacitation and sperm-*zona pellucida* binding (Fig. 5d, e, f).
286 The highlights of our study were the detection of enzymatic production of H_2S and its consequences
287 in the form of $-(S)_nH$ in mammalian spermatozoa. We detected H_2S in the sperm flagella of mice (Fig.
288 4e), humans (Fig. 5c), and boar (Fig. 5d). Moreover, we immunodetected all H_2S-releasing enzymes
289 in all models used in sperm flagellum; therefore, we indirectly related endogenous H_2S production to
290 its enzymes. Subsequently, we followed $-(S)_nH$ as a major result of H_2S action. To the best of our
291 knowledge, for the first time, we described and characterized proteins that underwent $-(S)_nH$ of cysteine
292 in spermatozoa. Protein persulfidation ($-(S)_nH$) was strictly located in the sperm midpiece (Fig. 4f),
293 which highly corresponds to H_2S occurrence and the location of its enzymes. These observations are
294 consistent with H_2S properties; although H_2S diffuses well across membranes, its short half-life, which
295 lasts a few seconds, a maximum of minutes[18], does not allow it to sufficiently affect proteins over long
296 distances. To further elucidate the role of $-(S)_nH$ in sperm physiology, we detected $-(S)_nH$ depending
297 on the live/dead status of human spermatozoa (Fig. 6). Surprisingly, live and dead spermatozoa did not
298 differ from each other in terms of $-(S)_nH$ (Fig. 6a, b). Because cell death is accompanied by a decrease
299 in pH, H_2S could be released from pH unstable iron-sulfur complexes located in mitochondria, thereby
300 maintaining the $-(S)_nH$ of nearby proteins even after cell death. To label -SH and $-(S)_nH$, we used the
301 affinity of iodoacetamidofluorescein (IAF) to the -SH group. IAF was previously used in a study that
302 addresses the quality of cryopreserved bull spermatozoa depending on -SH content[19]. Based on IAF
303 staining, the researchers distinguished several patterns, whose distribution was dependent on sperm
304 viability. Spermatozoa labelled strictly in the midpiece were associated with higher viability than
305 spermatozoa labelled along its entire length, as was the case in our study. Interestingly, the pattern
306 associated with viable spermatozoa is strikingly similar to the pattern of $-(S)_nH$. It is possible that viable
307 spermatozoa contain $-(S)_nH$ in their midpiece instead of free -SH, as was previously suggested[19]. If so,
308 $-(S)_nH$ located specifically in the mitochondrial sheath may play an important role in sperm metabolism
309 and redox defence. We supported this statement by identifying $-(S)_nH$ using mass spectrometry. In
310 most cases, the identified proteins were associated with mitochondrial metabolism and flagellar
311 movement (Fig. 6e). Some of these proteins have been reported to undergo $-(S)_nH$, including
312 glyceraldehyde-3-phosphate dehydrogenase, tubulin[16] and L-lactate dehydrogenase[4], but we were the
313 first to observe that these proteins were persulfidated in human spermatozoa. Some persulfidation
314 targets were previously discovered as S-nitrosylated, including A-kinase anchor protein, heat shock
315 protein and semenogelin[10], which supports the finding that S-nitrosylation serves as a $-(S)_nH$
316 precursor[4,5,20]. All these results prove that spermatozoa contain many proteins containing reactive
317 cysteine through which proteins can be easily turned on and off by redox PTMs.
318
319 Spermatozoa are completely dependent on previously produced proteins once they leave the male
320 reproductive tract; therefore, they are vulnerable to oxidative stress. Persulfidation could play a key
321 role in this context because it prevents cysteine hyperoxidation and thus stops redox signalling pathway
322 disruption and protein damage. The reducing abilities of H_2S could be essential during sperm
323 capacitation. As is known, capacitation is enhanced by reactive oxygen and nitrogen species, but
324 overproduction of these reactive species leads to oxidative stress and cell death[21–23]. However, H_2S,
325 through persulfidation, could contribute to the maintenance of redox balance, and thus prevent
326 premature capacitation, which is an often problem of sperm manipulation *in vitro* conditions (*e.g.* cell
327 maintenance *in vitro*, cryopreservation). In this study, we provided evidence for the enzymatic
328 production of H_2S not only in the testis but also in spermatozoa. We detected CBS, CTH and MPST in
329 mammalian spermatozoa and thus indirectly linked H_2S with its enzymes. We visualized H_2S and

330 therefore were able to localize it to the sperm flagella, where it affects nearby proteins by
331 persulfidation. We identified some persulfidated proteins seemingly crucial for sperm viability, and we
332 outlined the impact of endogenous H_2S production on male reproduction. We proved the existence of
333 H_2S-releasing enzymes, H_2S, and persulfidation and considered the link between them in spermatozoa.
334 Obviously, other sophisticated models of *in vitro* pharmacological treatment of sperm and/or targeted
335 silencing of all H_2S-releasing enzymes in somatic cells are needed for the achievement of experimental
336 data leading to a comprehensive acknowledgement of H_2S in the physiology of reproduction.
337 Moreover, there is no doubt that H_2S is an important signalling molecule that purposeful modulation
338 deserves a knowledge transfer to different medical disciplines.
339
340 **Methods**
341 All chemicals were purchased from Sigma Aldrich unless specified otherwise. Peanut agglutinin from
342 *Arachis hypogaea* (PNA) conjugated with Alexa Fluor™ 488 was purchased from Thermo Fischer
343 Scientific (MA, USA, #L21409). The primary polyclonal antibodies anti-cystathionine β-synthase
344 (anti-CBS), anti-cystathionine γ-lyase (anti-CSE) and anti-3-mercaptopyruvate sulfurtransferase (anti-
345 3MPST) as well as the secondary antibody goat anti-rabbit-Alexa Fluor® 647 (# ab150079) were
346 purchased from Abcam (Cambridge, UK).

347 **Animals, samples, and ethical statements.** C57Bl/6 male mice aged 21 days and 12-14 weeks as well
348 as all applied protocols as noted below were used in animal experiments, in accordance with the
349 Protection of Animals against Cruelty (Act No. 246/1992 Coll.) of the Czech Republic and under the
350 supervision of the Animal Welfare Advisory Committee at the Ministry of Education, Youth, and
351 Sports of the Czech Republic (approval number: MSMT-249/2017-4). Alternatively, boar ejaculates
352 were purchased from Chovservis Co. (Hradec Kralove, Czech Republic). Reports concerning
353 experimental animals follow the recommendations in the ARRIVE guidelines[24]. Human semen
354 samples were obtained after informed consent at the IVF Zentren Prof. Zech – Pilsen, Ltd. (Pilsen,
355 Czech Republic); the study of human sperm was approved by the Ethics Committee of Charles
356 University, Faculty of Medicine in Pilsen (238/2016). All methods were carried out in accordance with
357 relevant guidelines and regulations (WHO manual 2010[25]).

358 **Preparation of sperm samples.** Mouse spermatozoa isolated from the cauda epididymis were allowed
359 to swim out to human tubal fluid medium with HEPES (HTF-HEPES, LifeGlobal™, LifeGlobal
360 Group, USA). Ejaculated boar spermatozoa were diluted with Beltsville Thaw Solution (BTS) at a
361 concentration of 10 mil/ml and stored at 18 °C for two days until utilization for the *zona pellucida*-
362 binding assay. The rest of the boar spermatozoa were washed and resuspended in modified Tyrode's
363 lactate-HEPES medium (TL-HEPES)20,19 at a concentration of 10 mil/ml. For capacitation,
364 spermatozoa were resuspended in capacitated modified TL-HEPES medium20,19 at a concentration
365 of 10 mil/ml and allowed to capacitate for 4 h at 37 °C. Capacitated spermatozoa were then washed
366 from the capacitating medium and resuspended in noncapacitating modified TL-HEPES. Human
367 ejaculates, obtained from three normozoospermic aged 30 – 35, were processed according to the WHO
368 manual 2010[27]. Briefly, ejaculates were divided into the noncapacitated and capacitated groups.
369 Spermatozoa were allowed to swim up from ejaculates into HTF-HEPES medium, which was placed
370 over the ejaculate, for 2.5 h in a 37 °C water bath. In the case of the capacitated group, HTF-HEPES
371 medium was enriched with 0.3% bovine serum albumin (BSA). Thereafter, all samples were processed
372 according to the purpose stated below.

373 **Porcine *zona pellucida*-binding assay.** Pig oocytes were obtained from ovaries of 6- to 8-month-old
374 noncycling gilts (a crossbreed of Landrace x Large White), yielded at the slaughterhouse (Jatky Český
375 Brod a.s., Český Brod, Czech Republic). First, cumulus-oocyte complexes were collected from ovarian

376 follicles with a diameter of 2–5 mm by aspiration with a 20-gauge needle and handled in TL-HEPES-
377 medium supplemented with 0.1 mg/ml polyvinyl alcohol (PVA). Immature oocytes were matured *in*
378 *vitro* in modified tissue culture medium (mTCM; Gibco, Life Technologies, UK), as described
379 earlier21. After 44 h of culture, cumulus cells were removed with 0.1% hyaluronidase, and matured
380 oocytes with extruded polar bodies were selected for the binding assay. Spermatozoa stored in BTS
381 medium were washed and resuspended in modified Tris-buffered medium (mTBM; Abeydeera et al.,
382 1998) at a concentration of 1 mil/ml. Subsequently, 100,000 spermatozoa were added to oocyte-free
383 zonas and coincubated in 0.5 ml of mTBM at 39 °C and CO_2 for 30 min. Thereafter, *zona pellucida*-
384 bound spermatozoa were washed in PBS supplemented with PVA, fixed in 4% paraformaldehyde
385 (PFA) enriched with 0.1% Triton TX-100 and 1 mM DTT for 15 minutes at 37 °C, washed and stored
386 in PBS with sodium azide at 4 °C for immunocytochemistry.

387 **Immunocytochemistry.** Mouse, boar, and human spermatozoa were fixed and stored as described
388 above. Then, spermatozoa were allowed to adhere to polylysine-coated coverslips, permeabilized with
389 0.1% Triton TX-100 for 40 min, and blocked with 0.1% Triton TX-100–10% normal goat serum
390 (NGS)-1% BSA for 1 h at 37 °C. Subsequently, they were incubated with anti-CBS, anti-CSE and anti-
391 3MPST antibodies diluted 1:100 at 4 °C overnight. Thereafter, coverslips were washed, followed by
392 incubation with secondary antibody diluted 1:200 for 40 min at room temperature. PNA diluted 1:200
393 was added to the secondary antibody to follow the acrosome reaction. Coverslips were washed and
394 mounted in Vectashield® medium with 4'6'-diamino-2-phenylindole (DAPI; Vector Laboratories, Inc.,
395 CA, USA). Images were acquired using an Olympus IX83 fluorescence microscope (Olympus,
396 Germany) and VisiView® software (Visitron Systems GmbH, Germany).

397 **Immunofluorescence of mouse testes.** Mouse testes were fixed in 4% PFA, embedded in paraffin
398 wax with random orientation, and sectioned completely into 10-µm-thick slides. After
399 deparaffinization, antigen retrieval was performed using preheated citrate buffer (pH 6.0). Thereafter,
400 cross-sections were permeabilized with 0.1% Triton TX-100 for 40 min and blocked with 0.1% Triton
401 TX-100–10% NGS-1% BSA for 1 h at 37 °C. Subsequently, they were incubated overnight at 4 °C
402 with antibodies at the following dilutions: anti-CBS: 1:250, anti-CTH: 1:125, and anti-3-MPST: 1:150.
403 In the case of CBS and CTH, slides were incubated with the preadsorbed secondary antibodies anti-
404 rabbit-Alexa Fluor® 647 (1:200, Abcam, Cambridge, UK, # ab150083) and PNA. For 3-MPST
405 detection, slides were incubated with biotin-conjugated goat anti-rabbit antibody (1:200, # ab6720) for
406 40 min, washed and incubated with a cocktail of Alexa Fluor® 647-conjugated streptavidin (1:500,
407 Bioss, USA, # bs-0437R-A647) and PNA. Subsequently, the slides were washed, mounted and
408 visualized as described above.

409 **Probe detection of H_2S in spermatozoa.** Epididymal mouse, ejaculated boar and human spermatozoa
410 were resuspended in HTF-HEPES and TL-HEPES media, respectively, at a concentration of 2 mil/ml.
411 Working solutions were prepared with adequate medium containing 500 µM acetyl
412 trimethylammonium bromide (CTAB) and Sulfane Sulfur Probe 4 (SSP4) (SulfoBiotics, Dojindo EU
413 GmbH, Munich, Germany) dissolved in DMSO at a concentration of 1:500. In the negative control,
414 the SSP4 probe was omitted, and DMSO at the same concentration as SSP4 was used. For a positive
415 control, spermatozoa were coincubated with pyridoxal-5'-phosphate (PxP) at a concentration of 50 mM
416 for 30 min before incubation with the SSP4 probe. Subsequently, 200 µl of working solution and 5 µl
417 of sperm suspension were added to polylysine-coated coverslips and incubated for 15 min at 37 °C,
418 followed by slide mounting in PBS with Hoechst 33352 (1:1,000`Sigma-Aldrich, MO, USA) and
419 immediate evaluation.

420 **Colorimetric detection of H_2S in testicular tissue.** The enzymatic capacity to release H_2S was
421 assessed using a colorimetric approach as described earlier22, with slight modifications. Mouse
422 testicular tissue was homogenized in extraction buffer (1% $Zin(OAc)_2$, 20 mM EDTA, 50 mM Tris-
423 HCl, pH 8), enriched with Complete Mini Protease Inhibitor Cocktail® (Roche, Basel, Switzerland),
424 and lysed for 20 min on ice. After centrifugation, the lysate was incubated with 2 mM PxP and 10 mM
425 L-cysteine for 2 h at 37 °C in a N_2 atmosphere. Lysates without PxP and/or L-cysteine, a cofactor of
426 enzymes (CBS, CTH) and enzyme (CBS, CTH, MPST) substrate, respectively, were used as negative
427 controls. Thereafter, proteins were precipitated with 12.5% trichloroacetic acid for 10 min, and the
428 reaction was centrifuged. To 100 µl of the supernatant, 100 µl of 20 mM DMPE and 100 µl of $FeCl_3$
429 were added and incubated for 10 min, and the absorbance was read at 670 nm. The absorbance was
430 recalculated based on the standard curve of $Na_2S.9H_2O$, an exogenous H_2S donor, and is expressed as
431 nM H_2S.mg of tissue^{-1}.min^{-1}.

432 **Western blot.** Mouse testicular tissue, epididymal mouse spermatozoa and ejaculated boar and human
433 spermatozoa were washed two times with TBS, and the pellets were dissolved in RIPA lysis buffer23
434 with 100 mM DTT, enriched with Complete Mini Protease Inhibitor Cocktail (Roche, Switzerland)
435 and incubated for 30 min on ice. Thereafter, samples were subjected to sodium dodecyl sulfate
436 polyacrylamide gel electrophoresis (SDS-PAGE) on a 4–15% separating Mini-PROTEAN® precast
437 gel and blotted using a Trans-Blot Turbo Transfer System onto PVDF membranes (Bio-Rad
438 Laboratories, France). The membranes were blocked in 5% BSA in TBS with 0.05% Tween-20 (TBS-
439 T) for 60 min at room temperature. The membrane was incubated with primary antibodies as mentioned
440 above and diluted 1:1,000 in 1% BSA in TBS-T overnight at 4 °C. A rabbit monoclonal anti-histone
441 H3 antibody (1:1,000, Abcam, Cambridge) was used as the internal control. Horseradish peroxidase-
442 conjugated anti-rabbit IgG antibody (1:15,000; Invitrogen, Carlsbad, CA, USA) was applied for 60
443 min at room temperature. Target proteins were visualized using ECL Select Western Blotting Detection
444 Reagent® (GE Healthcare Life Sciences, UK) and a ChemiDoc® MP System (Bio-Rad).

445 **6-iodoacetamidofluorescein (6-IAF) switch assay.** Persulfidated proteins were visualized in
446 spermatozoa using a modified switch assay. First, spermatozoa were subjected to a LIVE/DEAD
447 Fixable Dead Cell Stain Kit (Invitrogen Life Technologies, Carlsbad, CA, USA, #L23105) as
448 previously described24. Persulfidation (- $(S)_nH$) and free thiols (-SH) were distinguished in accordance
449 with[16]. Briefly, free thiols of spermatozoa were blocked by 20 mM methyl methanethiosulfonate
450 (MMTS, Sigma-Aldrich, MO, USA, #64306) dissolved in HEN buffer (250 mM HEPES-NaOH (pH
451 8), 1 mM EDTA, and 0.1 mM neocuproine) for 60 min at 38 °C on a shaker. After blocking, the sperm
452 suspension was washed three times with PBS for 10 min on a shaker and centrifuged (300 g). Presumed
453 - $(S)_nH$ in spermatozoa was stained with 0.04 µM 6-iodoacetamidofluorescein (6-IAF, Thermo Fisher,
454 USA, #I30452) for 15 min at room temperature and fixed in 3.2% PFA for 10 min. The prepared
455 samples were analysed using a BD FACS Aria fusion cell analyser (Becton Dickinson, Prague, Czech
456 Republic) for flow cytometry. Data were collected from 5,000 events. LIVE/DEAD Fixable Dead Cell
457 Stain and 6-IAF were excited by 405 and 488 nm lasers and detected with 450/50 and 530/30 bandpass
458 filters. Acquired data were analysed using FlowJo software (Becton Dickinson, Prague, Czech
459 Republic). Alternatively, spermatozoa were settled down to coverslips, and - $(S)_nH$ was visualized *in*
460 *situ* via an Olympus IX83 fluorescence microscope (Olympus, Germany).

Biotin switch method and pulldown assay of human sperm and mouse testis, liver and brain. Detection of - $(S)_nH$ in lysate was processed as previously described[16] with slight modifications. Briefly, tissues were lysed in 100 µL of HENS buffer (250 mM HEPES-NaOH (pH 8), 1 mM EDTA, and 0.1 mM neocuproine, 1% SDS) and incubated on a shaker for 30 min. Then, lysates were centrifuged (10,000 g), 50 µL of supernatant was mixed with 150 µL of HEN buffer, and 0.38 µL of MMTS was added (reaching a final concentration of 20 mM). Free thiols in protein lysate were blocked for 20 min at 50 °C on a shaker. The residue of MMTS was then removed by ethyl acetate extraction, vortexed three times followed by brief centrifugation and ethyl acetate removal by pipette, followed by vacuum evaporation. The samples were labelled with the final concentration 3,3 mM EZ-linked iodoacetyl-PEG_2-biotin (Thermo Fisher, USA; #21334) overnight at 4 °C on a shaker. An aliquot of treated proteins was diluted in Laemmli loading buffer under reducing agent-free conditions; samples were separated by SDS-ELFO and visualized by Western blotting as described above using HRP-conjugated streptavidin (1:1,000; Sigma-Aldrich, MO, USA; #18-152) and chemiluminescence detection as described previously. Alternatively, lysates were loaded onto streptavidin-coated agarose beads (Millipore, MA, USA; #16-126) and incubated overnight at 4 °C on a shaker. Beads were treated with 100 mM β-mercaptoethanol in 4% SDS, and primary persulfidated proteins were eluted. The purified samples were processed for nano-LC-MS as described below.

Nano-LC-MS. Tissue lysates from animals and human spermatozoa were used for complete proteomic analysis. Nanoliquid chromatography-MS (nano-LC–MS) was used for protein identification and quantification, as described previously25.

Statistics. Data were analysed using GraphPad Prism 8 (GraphPad Software, Inc., San Diego, CA, USA). Based on Shapiro-Wilks normality distribution tests, differences were tested as noted below. P values ≤ 0.05, .01, .001, and .0001 were considered statistically significant and are indicated with asterisks (*), (**), (***), and (****), respectively.

Conflict of Interest. The authors have declared no conflict of interest.

Author Contributions. HŘ, MŠ, JN: experimental design, experimental work, data analysis, and manuscript preparation. JM: experimental work, data analysis. LM, JH, TF, ŠP, TŽ: experimental work, PH: phylogenetic tree and statistical analysis. JP, MK: manuscript preparation.

Funding. This study was supported by the project no. CZ.02.1.01/0.0/0.0/16_019/0000787 "Fighting Infectious Diseases", awarded by MEYS CR, Charles University Research Fund (Progres Q39), the Czech Health Research Council (grant no. NV18–01-00544); the National Sustainability Programme I (NPU I) Nr. LO1503 provided by the Ministry of Education, Youth and Sports of the Czech Republic (MEYS CR); the work was supported by the grant SVV–2020-2022 No 260 536 awarded by MEYS CR, and the United States Fulbright Commission (P001496).

Acknowledgments. We would like to thanks IVF Zentren Prof. Zech - Pilsen Ltd. (Pilsen, Czech Republic) and Mgr. Lukáš Gold for the human samples collection. Furthermore, our thanks belong to Ing. Lucia Maršálová for her kind help with testes slides preparation.

Reference

1. Aitken, R. J. Reactive oxygen species as mediators of sperm capacitation and pathological damage. *Molecular Reproduction and Development* **84**, 1039–1052 (2017).

501 2. Machado-Oliveira, G. *et al.* Mobilisation of Ca2+ stores and flagellar regulation in human
502 sperm by S-nitrosylation: A role for NO synthesised in the female reproductive tract.
503 *Development* **135**, 3677–3686 (2008).

504 3. O'Flaherty, C. Redox regulation of mammalian sperm capacitation. *Asian Journal of*
505 *Andrology* **17**, 583 (2015).

506 4. Fu, L. *et al.* Direct Proteomic Mapping of Cysteine Persulfidation. *Antioxidants and Redox*
507 *Signaling* **33**, 1061–1076 (2020).

508 5. Longen, S. *et al.* Quantitative Persulfide Site Identification (qPerS-SID) Reveals Protein
509 Targets of H2S Releasing Donors in Mammalian Cells. *Scientific Reports* **6**, 1–12 (2016).

510 6. Wood, Z. A., Schröder, E., Harris, J. R. & Poole, L. B. Structure, mechanism and regulation of
511 peroxiredoxins. *Trends in Biochemical Sciences* vol. 28 32–40 (2003).

512 7. Sun, J., Steenbergen, C. & Murrhy, E. S-Nitrosylation: NO-Related Redox Signaling to
513 Protect Against Oxidative Stress. *Antioxid Redox Signal.* **8**, 1693–1705 (2006).

514 8. Dóka *et al.* Control of protein function through oxidation and reduction of persulfidated states.
515 *Science Advances* **6**, (2020).

516 9. Petrovic, D., Kouroussis, E., Vignane, T. & Filipovic, M. R. The Role of Protein
517 Persulfidation in Brain Aging and Neurodegeneration. *Frontiers in Aging Neuroscience* **13**, 1–
518 12 (2021).

519 10. Lefièvre, L. *et al.* Human spermatozoa contain multiple targets for protein S-nitrosylation: An
520 alternative mechanism of the modulation of sperm function by nitric oxide? *Proteomics* **7**,
521 3066–3084 (2007).

522 11. Li, G., Xie, Z. Z., Chua, J. M. W., Wong, P. C. & Bian, J. Hydrogen sulfide protects testicular
523 germ cells against heat-induced injury. *Nitric Oxide - Biology and Chemistry* **46**, 165–171
524 (2015).

525 12. Wang, J. *et al.* Hydrogen Sulfide As a Potential Target in Preventing Spermatogenic Failure
526 and Testicular Dysfunction. *Antioxidants & Redox Signaling* ars.2016.6968 (2017)
527 doi:10.1089/ars.2016.6968.

528 13. Zhang, Y. *et al.* Hydrogen Sulfide, the Next Potent Preventive and Therapeutic Agent in
529 Aging and Age-Associated Diseases. *Molecular and Cellular Biology* **33**, 1104–1113 (2013).

530 14. Pintus, E., Jovičić, M., Kadlec, M. & Ros-Santaella, J. L. Divergent effect of fast- and slow-
531 releasing H2S donors on boar spermatozoa under oxidative stress. *Scientific Reports* **10**, 6508
532 (2020).

533 15. Zhang, W. *et al.* Decrease in male mouse fertility by hydrogen sulfide and/or ammonia can Be
534 inheritable. *Chemosphere* **194**, 147–157 (2018).

535 16. Mustafa, A. K. *et al.* HS signals through protein S-Sulfhydration. *Science Signaling* **2**, (2009).

536 17. Gao, D. D. *et al.* Cellular mechanism underlying hydrogen sulfide mediated epithelial K+
537 secretion in rat epididymis. *Frontiers in Physiology* **10**, (2019).

538 18. Polhemus, D. J. & Lefer, D. J. Emergence of Hydrogen Sulfide as an Endogenous Gaseous
539 Signaling Molecule in Cardiovascular Disease. *Circulation research* **114**, 730 (2014).

540 19. Chatterjee, S., de Lamirande, E. & Gagnon, C. Cryopreservation alters membrane sulfhydryl
541 status of bull spermatozoa: Protection by oxidized glutathione. *Molecular Reproduction and*
542 *Development* **60**, 498–506 (2001).

543 20. Finelli, M. J. Redox Post-translational Modifications of Protein Thiols in Brain Aging and
544 Neurodegenerative Conditions—Focus on S-Nitrosation. *Frontiers in Aging Neuroscience* **12**,
545 1–21 (2020).

546 21. Aitken, R. J. Reactive oxygen species as mediators of sperm capacitation and pathological
547 damage. (2017) doi:10.1002/mrd.22871.

548 22. Aitken, R. J. The Capacitation-Apoptosis Highway: Oxysterols and Mammalian Sperm
549 Function. *BIOLOGY OF REPRODUCTION* **85**, 9–12 (2011).

550 23. O'flaherty, C. & Matsushita-Fournier, D. Reactive oxygen species and protein modifications
551 in spermatozoa †. *Biology of Reproduction* **97**, 577–585 (2017).

552 24. Kilkenny, C., Browne, W. J., Cuthill, I. C., Emerson, M. & Altman, D. G. Improving
553 bioscience research reporting: The arrive guidelines for reporting animal research. *PLoS*
554 *Biology* **8**, (2010).

555 25. World Health Organization. *WHO laboratory manual for the examination and processing of*
556 *human semen.* (World Health Organization, 2010).

557 26. Kerns, K., Zigo, M. & Sutovsky, P. Zinc: A Necessary Ion for Mammalian Sperm Fertilization
558 Competency. *International Journal of Molecular Sciences* **19**, 4097 (2018).

559 27. World Health Organization. *WHO laboratory manual for the examination and processing of*
560 *human semen.* (World Health Organization, 2010).

561 28. Abeydeera, L. R., Wang, W. H., Cantley, T. C., Prather, R. S. & Day, B. N. Presence of β-
562 mercaptoethanol can increased the glutathione content of pig oocytes matured in vitro and the
563 rate of blastocyst development after in vitro fertilization. *Theriogenology* **50**, 747–756 (1998).

564 29. Xu, Z. *et al.* Ischemia-reperfusion reduces cystathionine-β-synthase-mediated hydrogen
565 sulfide generation in the kidney. *American Journal of Physiology - Renal Physiology* **297**,
566 (2009).

567 30. Zigo, M., Manaskova-Postlerova, P., Jonakova, V., Kerns, K. & Sutovsky, P.
568 Compartmentalization of the proteasome-interacting proteins during sperm capacitation.
569 *Scientific Reports* **9**, 1–18 (2019).

570 31. Ruiz-Díaz, S. *et al.* Changes in the cellular distribution of tyrosine phosphorylation and its
571 relationship with the acrosomal exocytosis and plasma membrane integrity during in vitro

572 capacitation of frozen/thawed bull spermatozoa. *International Journal of Molecular Sciences*
573 **21**, (2020).

574 32. Řimnáčová, H. *et al.* Low doses of Bisphenol S affect post-translational modifications of
575 sperm proteins in male mice. *Reproductive Biology and Endocrinology* **18**, (2020).

576

[1/03/2022]

Manuscript SREP-21-02368A

Responses to reviewers

Professor Ricardo Bertolla

Editorial Board Member, *Scientific Reports*

Dear Ricardo Bertolla,

Thank you for giving us the opportunity to submit a revised draft of our manuscript "Evidence of endogenously produced hydrogen sulfide (H_2S) and persulfidation in male reproduction" for publication in the Scientific Reports. We appreciate the time and effort that you and the reviewers dedicated to providing feedback on our manuscript and are grateful for the comments, which made our paper better. We have incorporated all of the suggestions made by the reviewers. Those changes are highlighted within the manuscript by tracked changes in the "Manuscript with changes marked" file and completely incorporated in the main Article File. Please see below, in italics, for a point-by-point response to the reviewers' comments and concerns.

Reviewer comments:

Reviewer #1 (Remarks to the Author): The manuscript by Rimnacova et al. describes the profile of hydrogen sulfide and persulfidation in male reproduction. The manuscript is technically sound and presents important observational data on the ability of the male reproductive tract in performing post-translational modification of proteins through production of hydrogen sulfide and persulfidation. Althought the presented data is an important contribution to the field, the consequences and role of hydrogen sulfide production and persulfidation are not explored in this manuscript and should be addressed either in this manuscript or in a subsequent publication perhaps through a inducible knock out of H2S producing enzymes. Nevertheless, this suggestion would greatly improve the manuscript, I also recognize that this would involve unattainable amount of work that would prevent the publication of this manuscript's important data and I would suggest a follow up work addressing the functional significance of these findings.
Please address this limitation in the manuscript.

Authors' response: *In our further, rather experimental work, we are achieving data underlining the reviewer's suggestions. Accordingly, concerning the breadth of this manuscript and other achieved findings, we decided to keep both sorts of data separate, followed by another submission of the mentioned experimental observations. This fact is newly claimed in the*

manuscript; please see lines 276-282 of the revised manuscript. Finally, the choice of experimental model is arduous because three enzymes release H_2S and, in accordance with their canonical expression, are substitutable. Designing of GM mouse strain should work on the triple-knock-out generation, strictly equipped with lox-flanked sequences (leading to spatiotemporal driving of gene excision). Triple KO using a cell population modulated with siRNA and/or CRISPR-Cas9 system seems more feasible; however, not bringing a solution for transcriptionally-silenced spermatozoa. We consider all these consequences within the planning of further experiments, and we will pay attention to all your comments.

Reviewer #2 (Remarks to the Author): The article entitled "Evidence of endogenously produced hydrogen sulfide (H2S) and persulfidation in male reproduction" by Hedvika Řimnáčová and colleagues aimed to verify the H2S action on testis and spermatozoa proteins, based on its releasing enzymes. The whole article is a very well-designed and complete study, answering an important question regarding the action of PTMs on spermatozoa. I have a few comments regarding some details:

1. I did not see any mention of the information on human samples. Are they normozoospermic ones, had some infertility problems or urogenital conditions. Age, weight, and other details are very important also.

Authors' response: *Information that analyzed spermatozoa belonging to normozoospermics was mentioned in the results (line 164). However, we also added this information into the Material and Methods section and the age of donors (line 312). Unfortunately, other information about donors has not been provided.*

2. Microscope configuration for each essay is missing

Authors' response: *In addition to existing details (lines 340-341) noted in M&M, we added the information about magnification into the appropriate figures (line 549, 555, and 562).*

3. Why do the authors use PNA to evaluate the acrosomal status and not PSA?

Authors' response: *PNA, as well as PSA, are lectins, binding to acrosome membrane. We used PNA because we have had good experience with this staining in our lab. It gives us more specific staining of acrosome than we got with PSA.*

4. What is the half-life of H_2S in spermatozoa and testicular tissue? Do the authors think that this evaluation is robust?

Authors' response: *This is a delicate question; H_2S half-life under in vivo conditions is extremely short, estimated between seconds to minutes (Polhemus & Lefer, 2014) (We added this information to the manuscript line 239). The presence of all three H_2S-releasing enzymes indicates continuous H_2S production, substitutability of these enzymes, and thus continuous supplementation of spermatozoa by H_2S. Together with its short half-life, this testifies to a very sophisticated regulatory mechanism, which has also been detected in other tissues. Nevertheless, technically in this manuscript: colorimetric assay has been used and, principally,*

the enzymatic capacity of H_2S-releasing enzymes is tested, using surplus of both cofactor and substrate, in the tissue lysate for 2 hrs. Therefore, we consider alternative approaches for the description of physiological capacity and genuine H_2S production in a tissue, being a part of upcoming experiments.

5. Why do the authors use Histone H3 and loading control? Do these proteins pass through persulfidation like GAPDH? We already know that methylation and other PTM occur in this protein.

Authors' response: *We use H3 as a loading control for western blot because the modifications we are seeking, including persulfidation, sulfenylation, and nitrosylation, do not modify histones abundantly (if at all); therefore, there is no interference of loading control and analyzed PTM assumed. Molecular weight (16 kDa) is another reason for choosing H3; otherwise, the stripping must be used for (e.g.) GAPDH detection. However, stripping decreases detection efficiency, and we prefer to avoid it. Moreover, histones are often biotinylated naturally* (Sidoli et al., 2012)*, and biotin-based detection does not seem to be a good approach for histone analyses.*

Editorial Board Member comments:

While both reviewers have acknowledged strenghts within the mauscript, there are minor points that authors need to address. Authors should particularly consider adding context as to the consequences of H2S and persulfidation to sperm, in the discussion. Moreover, technical information regarding H2S half-life is of particular interest, as there are many products of oxidation in semen that are evanescent, and it would be of interest to know if this is the case for H2S and persulfidation. Finally, did authors verify potential interaction with cysteine-rich proteins, such as sperm nuclear protamines?

Authors' response: *The consequences of the H_2S action were outlined in the lines 251 – 261 and 264 – 266, but we agree that the description is too general. That is why, we added more specific consequences of H_2S and persulfidation in lines 266 – 271.*

We also added information about H_2S half-life in lines 239. You are right, persulfidation, as well as other redox PTMs, including that arising from the oxidation reaction (nitrosylation, sulfenylation), are unstable and very dynamic. Therefore, we included a sentence in lines 197 – 198.

That is a very good point with protamines and H_2S. H_2S is a small liposoluble molecule that could easily pass-through membranes and reach tightly packaged sperm chromatin. Based on this, we assume the role of H_2S in disulfide bond reduction within protamines. However, the protamine isolation, which needs a large amount of reducing agents like DTT, is not compatible with biotin-switch assay (persulfidation detection) and, unfortunately, with any other assay available for persulfidation detection. However, the ability of H_2S to reduce disulfide bond and/or create persulfidation in protamines is a focus of our recent experiments and will be the theme of our future manuscript.

References:

Polhemus, D. J., & Lefer, D. J. (2014). Emergence of Hydrogen Sulfide as an Endogenous Gaseous Signaling Molecule in Cardiovascular Disease. Circulation Research, 114(4), 730. https://doi.org/10.1161/CIRCRESAHA.114.300505

Sidoli, S., Cheng, L., & Jensen, O. N. (2012). Proteomics in chromatin biology and epigenetics: Elucidation of post-translational modifications of histone proteins by mass spectrometry. Journal of Proteomics, 75(12), 3419–3433. https://doi.org/10.1016/J.JPROT.2011.12.029